

Cell Chemical Biology

A Small-Molecule Inhibitor of Bax and Bak Oligomerization Prevents Genotoxic Cell Death and Promotes Neuroprotection

Highlights

- Discovery of novel small-molecule inhibitors of Bax and Bak oligomerization
- Compounds provide evidence that monomeric Bax/Bak is insufficient for MOMP
- Compounds prevent Bax/Bak oligomerization at specific dimer sites
- Compounds prevent cell death and mediate neuroprotection after excitotoxicity

Authors

Xin Niu, Hetal Brahmbhatt,
Philipp Mergenthaler, ...,
Carsten Culmsee, Jing Yi,
David W. Andrews

Correspondence

david.andrews@sri.utoronto.ca

In Brief

Niu et al. identified novel small-molecule inhibitors of pro-apoptotic Bax and Bak oligomerization which allow cells to resist apoptosis and that protect neurons from excitotoxicity, providing novel tools for preclinical target evaluation and drug development in degenerative diseases.

A Small-Molecule Inhibitor of Bax and Bak Oligomerization Prevents Genotoxic Cell Death and Promotes Neuroprotection

Xin Niu,^{1,2,12} Hetal Brahmbhatt,^{1,3,12} Philipp Mergenthaler,^{3,4,5,12} Zhi Zhang,⁶ Jing Sang,^{2,3} Michael Daude,⁷ Fabian G.R. Ehlert,⁷ Wibke E. Diederich,⁷ Eve Wong,¹ Weijia Zhu,¹ Justin Pogmore,³ Jyoti P. Nandy,^{9,13} Maragani Satyanarayana,^{9,14} Ravi K. Jimmidi,^{11,15} Prabhat Arya,^{9,16} Brian Leber,^{1,10} Jialing Lin,⁶ Carsten Culmsee,⁸ Jing Yi,² and David W. Andrews^{1,3,17,*}

¹Department of Biochemistry and Biomedical Sciences, McMaster University, Hamilton, ON L8S 4L8, Canada

²Department of Biochemistry and Molecular Cell Biology, Institutes of Medical Sciences, Shanghai Jiao Tong University School of Medicine, Shanghai 200025, China

³Biological Sciences, Sunnybrook Research Institute, University of Toronto, Toronto, ON M4N 3M5, Canada

⁴Departments of Experimental Neurology and Neurology, Center for Stroke Research, NeuroCure Clinical Research Center, Charité – Universitätsmedizin Berlin, Charitéplatz 1, 10117 Berlin, Germany

⁵Berlin Institute of Health, 10117 Berlin, Germany

⁶Department of Biochemistry and Molecular Biology, Peggy and Charles Stephenson Cancer Center, University of Oklahoma Health Sciences Center, Oklahoma City, OK 73126, USA

⁷Department of Medicinal Chemistry, Center for Tumor Biology and Immunology, Philipps Universität Marburg, 35043 Marburg, Germany

⁸Fachbereich Pharmazie, Institut für Pharmakologie und Klinische Pharmazie, Philipps Universität Marburg, 35043 Marburg, Germany

⁹Drug Discovery Program, Ontario Institute for Cancer Research, MARS Centre, Toronto, ON M5G 0A3, Canada

¹⁰Department of Medicine, McMaster University, Hamilton, ON L8S 4L8, Canada

¹¹Reddy's Institute of Life Sciences, University of Hyderabad Campus, Gachibowli, Hyderabad 500046, India

¹²Co-first author

¹³Present address: Therapeutic Product Directorate, Health Canada, 101 Tunney's Pasture Driveway, Ottawa, ON K1A 0K9, Canada

¹⁴Present address: TCG Life Sciences, Bio Resource Center, Gensis Campus, Hinjewadi, Pune, Maharashtra 411057, India

¹⁵Present address: SAI Life Sciences Limited, unit-II, IKP knowledge Park, Shameerpet, Hyderabad 500078, India

¹⁶Present address: Dr. Reddy's Institute of Life Sciences, University of Hyderabad Campus, Gachibowli, Hyderabad 500046, India

¹⁷Lead Contact

*Correspondence: david.andrews@sri.utoronto.ca

<http://dx.doi.org/10.1016/j.chembiol.2017.03.011>

SUMMARY

Aberrant apoptosis can lead to acute or chronic degenerative diseases. Mitochondrial outer membrane permeabilization (MOMP) triggered by the oligomerization of the Bcl-2 family proteins Bax/Bak is an irreversible step leading to execution of apoptosis. Here, we describe the discovery of small-molecule inhibitors of Bax/Bak oligomerization that prevent MOMP. We demonstrate that these molecules disrupt multiple, but not all, interactions between Bax dimer interfaces thereby interfering with the formation of higher-order oligomers in the MOM, but not recruitment of Bax to the MOM. Small-molecule inhibition of Bax/Bak oligomerization allowed cells to evade apoptotic stimuli and rescued neurons from death after excitotoxicity, demonstrating that oligomerization of Bax is essential for MOMP. Our discovery of small-molecule Bax/Bak inhibitors provides novel tools for the investigation of the mechanisms leading to MOMP and will ultimately facilitate development of compounds inhibiting Bax/Bak in acute and chronic degenerative diseases.

INTRODUCTION

Apoptosis is a highly regulated form of programmed cell death that serves to remove superfluous cells during development and its balanced regulation is of fundamental importance for homeostasis in all organisms (Danial and Korsmeyer, 2004). However, different forms of acute stress such as ischemia, ischemia-reperfusion, inflammation, degenerative diseases, as well as cancer chemotherapy in normal tissues can lead to the pathologic activation of apoptotic cascades (Hardwick and Soane, 2013; Leber et al., 2010; Mergenthaler et al., 2004; Szeto, 2008).

Apoptosis can be largely divided into two connected pathways ultimately leading to caspase activation and subsequent cellular disintegration. The extrinsic pathway is triggered by extracellular signals activating death receptors, whereas the intrinsic pathway is activated by intracellular stress and largely regulated at the mitochondrial outer membrane (MOM) by the pro- and anti-apoptotic members of the B cell lymphoma 2 (Bcl-2) family of proteins (Bogner et al., 2010; Danial and Korsmeyer, 2004; Moldoveanu et al., 2014). Cancer cells have evolved many strategies to evade apoptosis (Delbridge et al., 2012), therefore, pharmacological inhibition of anti-apoptotic proteins has been studied in great detail. However, the therapeutic potential of pharmacological

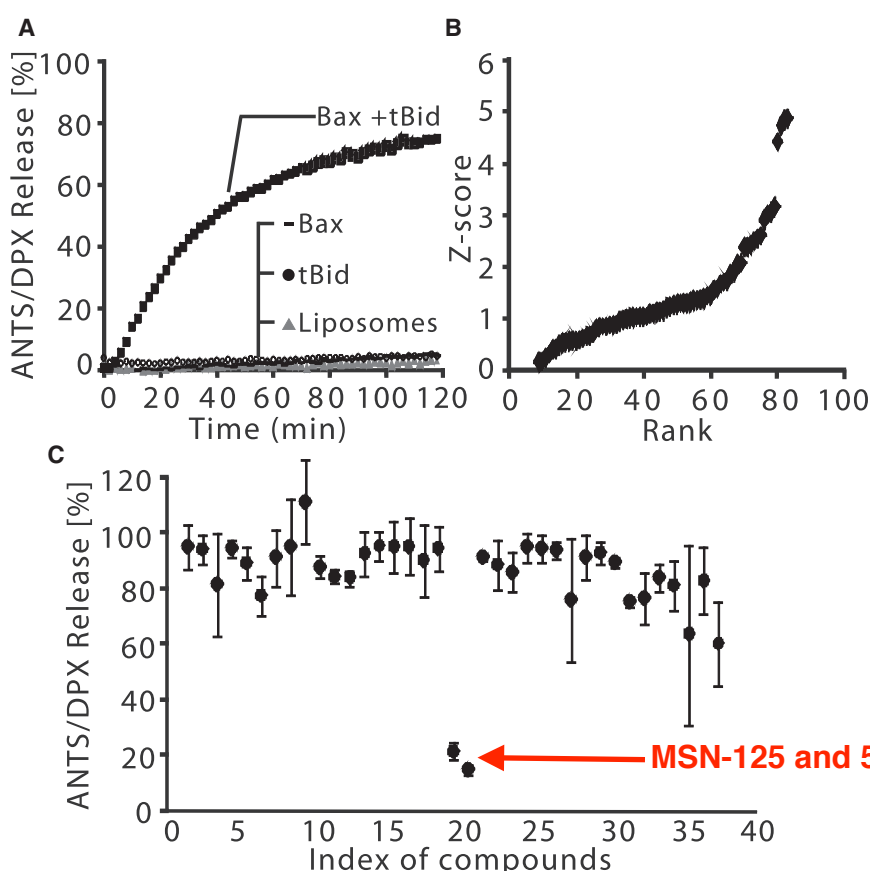


Figure 1. Identification of Inhibitors of tBid- and Bax-Mediated Liposome Permeabilization

(A) Bax (100 nM) and tBid (20 nM) permeabilize liposomes releasing ANTS and DPX, resulting in a fluorescence increase. Fluorescence increase is converted to percentage release by comparing to liposomes solubilized with detergent.

(B) Z score versus rank for 86 compounds screened in triplicate at 10 μ M final concentration. All compounds with a Z score > 0 for inhibiting tBid/Bax-mediated liposome permeabilization are shown.

(C) Primary ANTS/DPX release screen for 37 compounds designed based on BJ-1 and BJ-1-BP, the top hits from (B). MSN-125 and MSN-50 (index 19 and 20) inhibited liposome permeabilization normalized to dye release by tBid and Bax alone. Endpoint release was measured after incubation for 120 min, $n = 2$, mean \pm range. Unless otherwise specified in all figures, n indicates the number of independent experiments.

Bax and Bak protein complexes in the MOM have prohibited rational design of small-molecule inhibitors.

Here, we identified small-molecule inhibitors active against both Bax and Bak oligomerization in the MOM that also inhibit apoptosis in live cells. Using a combination of biochemical in vitro assays and cellular studies, we demonstrate

inhibition of pro-apoptotic Bcl-2 proteins has been less explored.

Mitochondrial outer membrane permeabilization (MOMP) is the first irreversible step in apoptosis (Delbridge et al., 2012; Moldoveanu et al., 2014; Willis et al., 2007). MOMP results from an ordered series of steps beginning with activation of one or more Bcl-2 homology 3 proteins (BH3-proteins) or releasing previously activated pro-apoptotic proteins Bax or Bak from inhibition by an anti-apoptotic protein of the Bcl-2 family (Bogner et al., 2010; Willis et al., 2007; Wilson-Annan et al., 2003). Once activated, BH3-proteins translocate to the MOM and directly recruit and activate cytoplasmic Bax and the constitutively membrane-bound Bak (Lovell et al., 2008; Sarosiek et al., 2013) catalyzing insertion of the central helices 5–6 of the proteins into the lipid bilayer of the MOM as part of a yet to be fully defined structure (Andrews, 2014). Some data suggest that oligomerization of membrane-bound Bax or Bak ultimately culminates in MOMP (Dewson et al., 2012; Iyer et al., 2015; Ma et al., 2013; Zhang et al., 2016). Other results have been interpreted as suggesting that MOMP can be mediated by membrane-inserted monomers of Bax (Kushnareva et al., 2012; Xu et al., 2013). Thus, MOMP could be prevented by inhibiting any one of the individual steps that lead to the activation of Bax and Bak in the MOM, or possibly by preventing the oligomerization of the proteins.

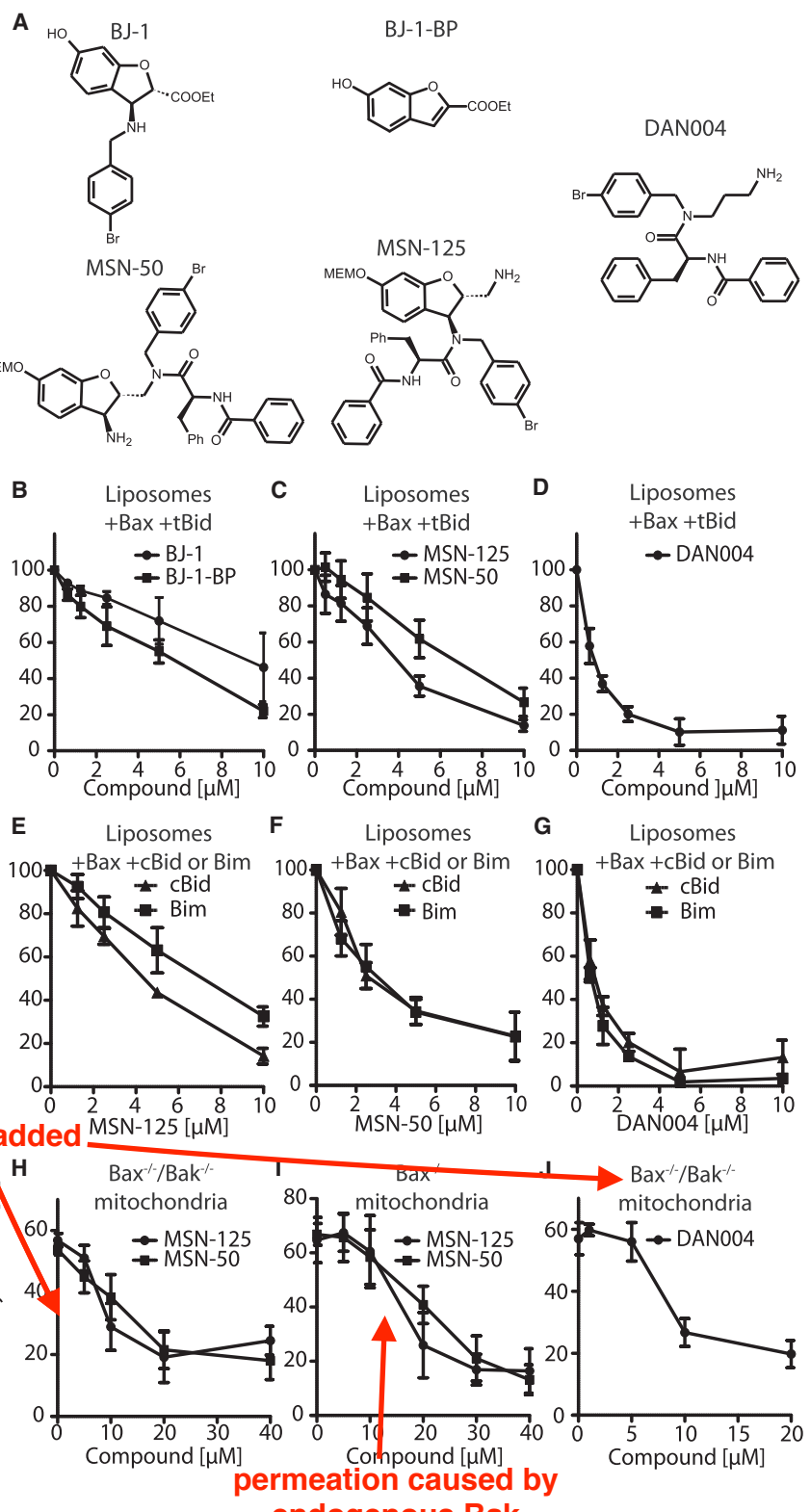
Multiple structurally disparate BH3 proteins mediate activation of Bax and Bak, therefore directly inhibiting Bax and Bak would be a more efficient approach to inhibit MOMP. However, the lack of structural information about and the overall dynamic nature of

a specific mechanism of action for these inhibitors. In structural crosslinking studies we demonstrate that these small molecules partially disrupt normal Bax and Bak dimerization at similar interfaces, thereby preventing dimers from forming higher-order oligomers, and thus establish that proper Bax/Bak dimerization is necessary for MOMP. Importantly, we demonstrate that pharmacological inhibition of Bax and Bak with these small molecules allows cells to survive otherwise lethal stress and rescues neurons from prior excitotoxic damage. Finally, our studies provide novel tools to investigate the molecular mechanisms underlying MOMP and lay the ground for accelerated targeted development of refined Bax and Bak inhibitors that may be used for preclinical target validation.

RESULTS

Identification of Small-Molecule Bax Inhibitors

To identify novel Bax inhibitors, we screened a collection of 86 compounds based on structures previously shown to have a weak affinity for Mcl-1 (Prakesch et al., 2008) for inhibition of tBid/Bax-mediated membrane permeabilization (MP) in a MOMP-mimicking liposome dye-release assay (Billen et al., 2008) (Figures 1A and 1B). A 37-compound secondary collection based on the molecular structures of the compounds with the highest activities in the primary screen (BJ-1 and BJ-1-BP) was again screened for inhibition of Bax-mediated MP. From this collection, both MSN-50 and MSN-125 efficiently inhibited liposome permeabilization (Figures 1C and 2A).



Small-Molecule Inhibition of Liposome Permeabilization by tBid and Bax Is Concentration Dependent

In individual assays, BJ-1, BJ-1-BP, MSN-50, and MSN-125 all inhibited dye release from liposomes in a concentration-dependent fashion (Figures 2B and 2C). Structure-activity relationship

Figure 2. Small-Molecule Inhibitors that Prevent Bax-Mediated Permeabilization of Liposomes and Mitochondria

(A) Molecular structures of BJ-1, BJ-1-BP, MSN-125, MSN-50, and DAN004. MEMO, β -methoxymethyl ether.

(B–D) Concentration-dependent inhibition of liposome permeabilization by tBid and Bax by the indicated concentrations of (B) BJ-1, BJ-1-BP, (C) MSN-125, MSN-50, and (D) DAN004. Results are normalized to reactions without compound. Mean \pm SD, n \geq 3.

(E–G) Liposome permeabilization by Bax activated by either 5 nM cBid or Bim is inhibited equally by the compound and concentrations indicated below the panels. Results are normalized to reactions without compound.

(H–J) Permeabilization of mitochondria isolated from (H and J) $Bax^{-/-}/Bak^{-/-}$ or (I) $Bax^{-/-}$ BMK cells expressing Smac-mCherry incubated with (H and J) 2 nM tBid and 20 nM Bax or (I) 0.5 nM tBid and compounds as indicated. Release of Smac-mCherry was determined by pelleting mitochondria and measuring mCherry fluorescence in the supernatant and pellet. Mean \pm SD, n \geq 3. See also Figure S1 and Table S1.

(SAR) experiments suggested that most modifications of MSN compounds significantly reduced their activity (Table S1). The BJ-1-BP structure is included in all of the hit compounds suggesting that this might be the pharmacophore. Unexpectedly, we found that only MSN-50 and MSN-125 inhibited liposome permeabilization by a common mechanism (see below). Therefore, to identify the pharmacophore common to these compounds, we synthesized DAN004 (Figure 2A). Like the parent compounds, DAN004 showed concentration-dependent inhibition of liposome permeabilization but with improved activity *in vitro* (Figure 2D).

This assay does not permit determination of conventional kinetic parameters since new oligomers form in liposomes that have already been permeabilized, and existing Bax oligomers can continue to expand until they contain hundreds of Bax molecules (Satsoura et al., 2012). Neither of these events is recorded in our assay as liposome permeabilization is an “all-or-nothing” event. Nevertheless, this assay permits derivation of concentration response curves, thereby allowing

quantitative comparison of different compounds under identical conditions. The concentration of compound required to inhibit 50% of the maximal dye release (i.e., IC₅₀) obtained for MSN-125, MSN-50, BJ-1, and BJ-1-BP in this assay were approximately 4, 6, 9, and 6 μ M, respectively (Figures 2B and 2C).

This does not mean that these ligand bind somewhere else. Only that they do not bind to BH3 protein.

DAN004 exhibited the most potent MP-inhibiting activity ($IC_{50} \sim 0.7 \mu M$, Figure 2D). Consistent with a previous report (Jiang et al., 2007), Nutlin-3a, a small-molecule inhibitor of MDM2, inhibited liposome permeabilization in a concentration-dependent fashion but was less active than DAN004 (Figure S1). MSN-125, MSN-50, and DAN004 inhibited activation of Bax mediated by either Bim or cBid more or less equivalently (Figures 2E–2G). Other than the BH3-sequence there is no structural similarity between these Bax activator-proteins consistent with the target of the inhibitors being Bax rather than the BH3 proteins. Moreover, DAN004 and Bcl-XL inhibited tBid-activated Bax-mediated liposome permeabilization equivalently (Figure S1I), further confirming that the compound does not function by inhibiting a BH3 protein. Finally, we took advantage of the fact that, when Bak is synthesized by in vitro transcription translation, the protein is constitutively active, releasing cytochrome c from mitochondria lacking endogenous Bax and Bak. Consistent with MSN-50 targeting Bak, adding the compound to constitutively active Bak prior to the addition of mitochondria reduced cytochrome c release, as measured by ELISA in three independent experiments, from 43% to 19%. By comparison, in vitro synthesized Bcl-XL, used as a control in the same experiments, inhibited active Bak-mediated cytochrome c release from 45% to 3%.

MSN-50, MSN-125, and DAN004 Inhibit Bax- and Bak-Mediated MOMP

To determine whether the compounds inhibited tBid-activated Bax and/or Bak in mitochondria, the compounds were added to permeabilization assays containing mitochondria isolated from $Bax^{-/-}$ or $Bax^{-/-}/Bak^{-/-}$ baby mouse kidney (BMK) cell lines stably expressing Smac-mCherry in the mitochondrial intermembrane space (Shamas-Din et al., 2014). Release of the fluorescence protein measured by fluorimetry provided a quantitative assessment of MOMP (Figures 2H and 2I). In control experiments, none of the compounds alone resulted in significant mitochondrial permeabilization even at 40 μM (Figure S1C). Therefore, this concentration was chosen as the maximum for the assays used to measure inhibition of Bax and Bak. Both MSN-50 and MSN-125 inhibited tBid/Bax-mediated MOMP in a concentration-dependent manner (Figure 2H). However, BJ-1 and BJ-1-BP failed to inhibit Bax-induced MOMP (Figure S1D) and Nutlin-3a only poorly inhibited tBid/Bax-mediated MOMP (Figure S1B). The activity of Nutlin-3a in preventing mitochondrial permeabilization was so poor that, similar to BJ-1 and BJ-1-BP, it would not be possible to ascribe any activity observed in cells to inhibition of Bax and therefore these compounds were not pursued further. The reasons why these compounds are not active with mitochondria are not clear but may be related to non-specific binding to mitochondria or metabolism by enzymes in the crude mitochondrial fractions known to contain peroxisomes and vesicles derived from the secretory pathway.

As expected, mitochondria from $Bax^{-/-}$ cells were efficiently permeabilized by tBid alone due to activation of endogenous Bak in the MOM and/or release of activated Bak from endogenous anti-apoptotic proteins (Figure 2I). It was not possible to measure the amount of endogenous Bak on the MOM with sufficient accuracy to quantitatively compare compound-mediated inhibition of Bak with inhibition of the known quantities of Bax added to $Bax^{-/-}/Bak^{-/-}$ mitochondria. Nevertheless, MSN-50,

MSN-125, and DAN004 showed concentration-dependent inhibition of Bak-mediated MOMP (Figures 2H–2J and S1F), whereas BJ-1 and BJ-1-BP did not show any activity in this assay (Figure S1E). Taken together the above results demonstrate that MSN-50, MSN-125, and DAN004 inhibit both Bax and Bak.

MSN-125 and MSN-50 Inhibit Apoptosis in Cells

To further characterize MSN-50, MSN-125, and DAN004 functionally, potency in inhibiting Bax/Bak-mediated apoptosis in human colon cancer (HCT-116) cells, BMK cells was investigated. To dissect the inhibition of Bax and Bak, wild-type (WT), $Bax^{-/-}$, $Bak^{-/-}$, and $Bax^{-/-}/Bak^{-/-}$ (DKO) HCT-116 cells and BMK cells were assayed for survival and proliferation after induction of apoptosis by treating these cells with actinomycin D (ActD) or staurosporine (STS). Since ActD and STS were added transiently and the cells allowed to recover for 4 days before replating, lack of growth indicates that the cells died. As expected, in the absence of the inhibitor compounds, only $Bax^{-/-}/Bak^{-/-}$ cells survived and proliferated after ActD or STS treatment and replating (Figures 3A–3C). Pre-treatment of the cells with 5 or 10 μM MSN-50 or MSN-125 conferred survival to ActD-treated WT, $Bax^{-/-}$ and $Bak^{-/-}$ HCT-116, and BMK cells (Figures 3A and 3C, respectively). Concentrations of 5 and/or 10 μM of the MSN compounds are shown because lower concentrations were largely ineffective, while concentrations of 20 μM or higher had off-target toxicity that killed HCT-116 and BMK DKO cells. Similar results were also obtained for BMK cells treated with STS. Although the results with STS were more variable, the data are also consistent with the compounds inhibiting both Bax and Bak (Figures 3A–3C). ILS-JRK-C95-182, a compound structurally similar to MSN-50 and MSN-125 that displayed only a minimal inhibitory effect in the liposome permeabilization assay (Table S1), also lacked protective activity in live cells (Figures 3A–3C). Control wells without ActD or STS treatment demonstrated that, when administered alone, 5 or 10 μM MSN-50 or MSN-125 had negligible effects on cell proliferation (Figure 3A).

DAN004 is toxic

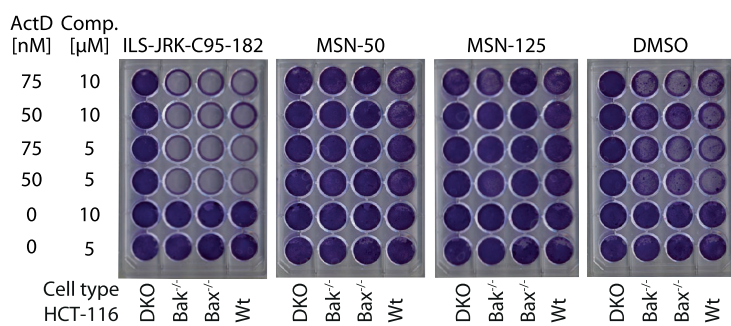
Although DAN004 exhibited potent inhibitory activity in vitro, it exhibited marked toxicity at 10 μM in cell-replating assays (Figure S2A). Furthermore, at sub-toxic doses DAN004 did not confer protection against ActD treatment (Figure S2B). Due to the large number of potential reasons for the off-target toxicity of DAN004 the compound was not pursued further here.

To correlate the functional inhibition of apoptosis by MSN-125 to inhibition of Bax in cells, we performed immunofluorescence with the conformation-specific anti-Bax-6A7 antibody that binds to an N-terminal epitope of Bax that is exposed after activation (Hsu and Youle, 1998). As expected, ActD treatment triggered endogenous Bax to adopt the 6A7-positive conformation and cytochrome c release from almost all mitochondria in HCT-116 WT cells (Figures 3D and S2C). Addition of MSN-125 prevented both Bax-6A7 positivity and cytochrome c release (Figure 3D), but not morphological changes in cells and mitochondria (Figure S2C), consistent with the compound inhibiting both Bax and Bak but not the original damage caused by ActD.

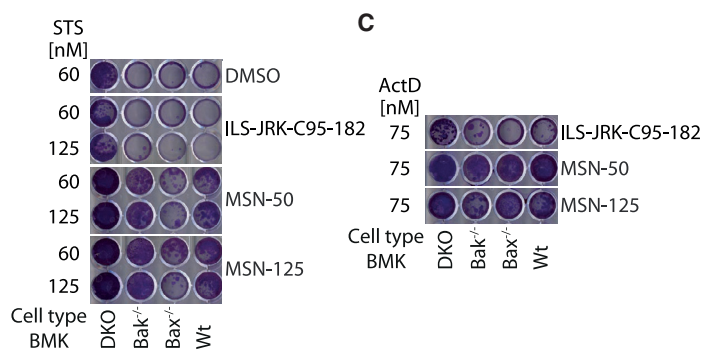
MSN-125 Protects Primary Neurons against Glutamate Excitotoxicity

Glutamate excitotoxicity can be mediated by Bax-dependent pathways (D'Orsi et al., 2012) and excessive release of

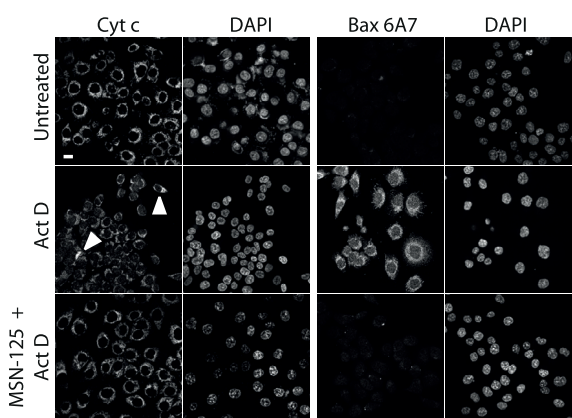
A



B



D



E

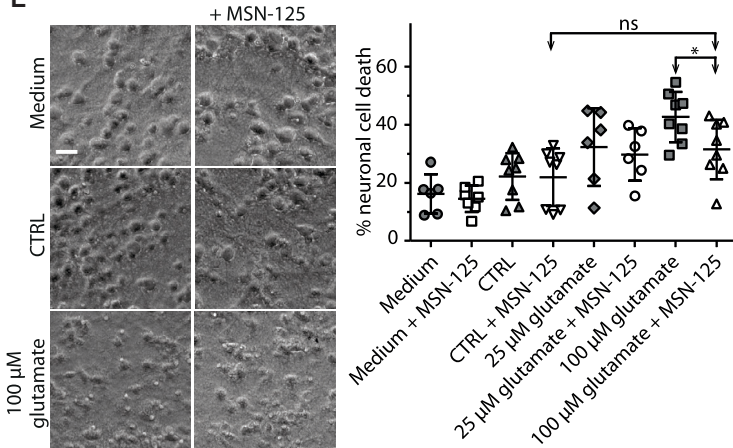


Figure 3. MSN-50 and MSN-125 Protect HCT-116 Cells, BMK Cells, and Primary Cortical Neurons from Apoptosis

(A–C) HCT-116 or BMK cell lines were incubated with the inhibitor specified above the panels and ActD or STS. After replating, viable cells were stained with crystal violet. See [STAR Methods](#) for details.

(A) MSN-50 and MSN-125 (5 and 10 μ M, indicated Comp.) but not the negative controls (ILS-JRK-C95-182, DMSO) conferred long-term survival and growth of HCT-116 cells exposed to actinomycin D (ActD).

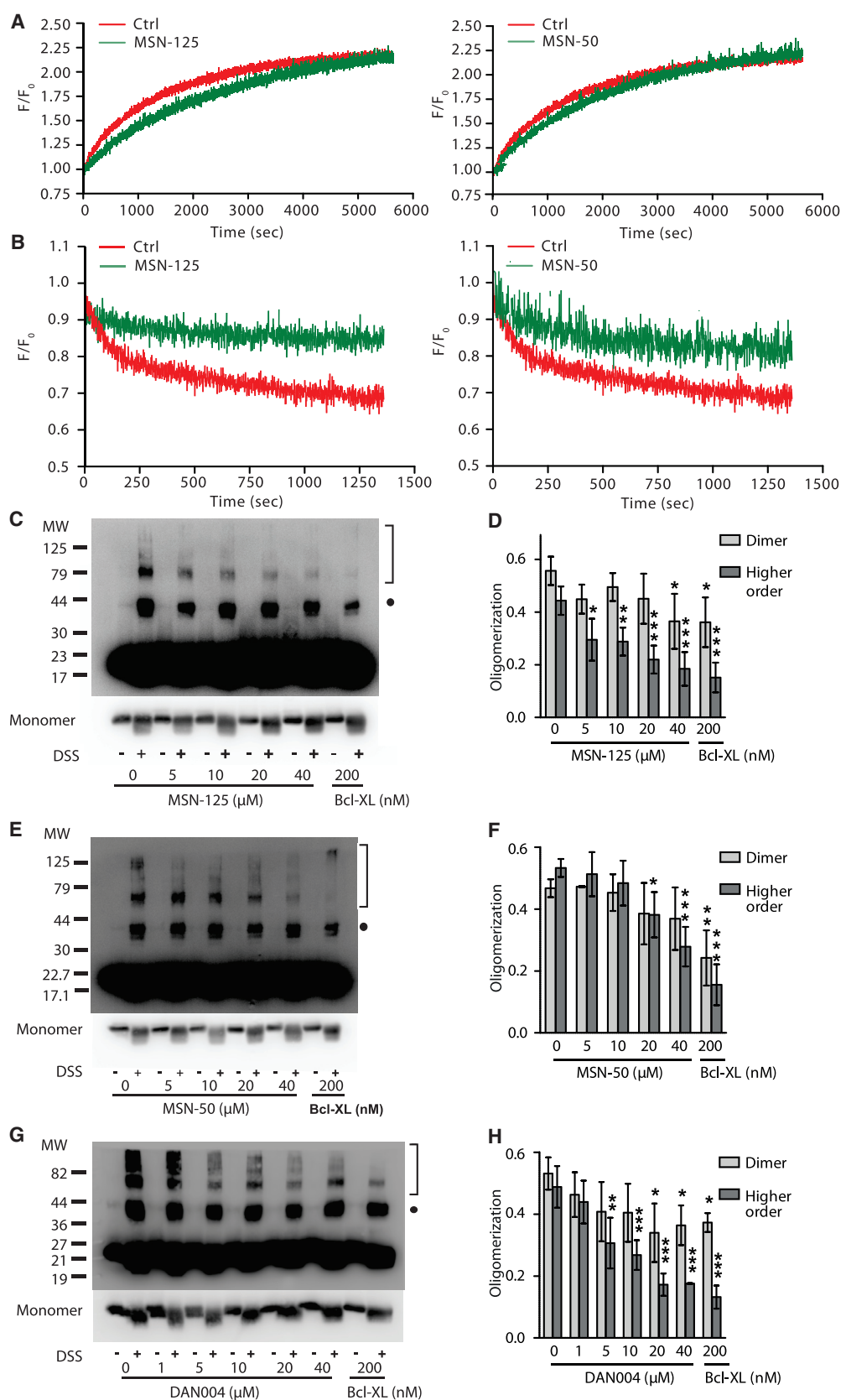
(B) MSN-125 and MSN-50 (5 μ M) conferred long-term survival and growth of BMK cells exposed to the indicated concentrations of STS.

(C) MSN-125 and MSN-50 (5 μ M) conferred long-term survival and growth of BMK cells exposed to 75 nM ActD.

(D) In cells treated with ActD, MSN-125 prevented exposure of the N-terminal 6A7 Bax epitope and cytochrome c release. HCT-116 cells were treated with 10 μ M MSN-125 for 3 hr before ActD treatment for 24 hr. Cells were fixed and immunofluorescence was performed with primary antibodies against activated Bax (6A7) or cytochrome c. Nuclei were visualized using DAPI. ActD treatment resulted in cytochrome c release from almost all cells. Two regions of mitochondria retaining cytochrome c in a field of ActD-treated cells are indicated with arrowheads. Scale bar, 10 μ m. See also [Figure S2C](#).

(E) MSN-125 (5 μ M) protected neurons from prior excitotoxic treatment with 100 μ M glutamate. Medium, continuous culture without wash; CTRL, neurons incubated in BSS₀. Phase-contrast images (left panels) and lactate dehydrogenase-release assay (right panel) are shown. Individual data points and mean \pm SD are displayed, n = 6–8 individual experiments. *p < 0.05, one-way ANOVA, Bonferroni post hoc; ns, not significant. Scale bar 25 μ m. See also [Figure S2](#).

FRET from DAC (on membrane) to NBD (on Bax) leads to fluorescence intensity increase



(legend on next page)

glutamate, as well as Bax-mediated apoptosis, contribute to neuronal cell death in stroke (D'Orsi et al., 2015; Mergenthaler et al., 2004). To determine whether MSN-125 would protect cultured primary embryonic mouse brain cortical neurons from glutamate excitotoxicity, neurons were treated with 25 or 100 μ M glutamate for 30 min, which led to substantial neuronal cell death after 24 hr (Figure 3E). However, treatment with 5 μ M MSN-125 directly after the excitotoxic insult substantially reduced neuronal damage. At this concentration and time point, treatment with MSN-125 alone did not result in neuronal damage. Thus, unlike other neuroprotective agents MSN-125-mediated inhibition of Bax and Bak protects neurons when administered after the excitotoxic insult. Collectively, these data validate Bax and/or Bak as potential therapeutic and druggable targets.

Molecular Mechanism of Small-Molecule Inhibition of Bax

Bax-mediated MOMP proceeds as an ordered series of steps including tBid binding to the MOM, recruitment of Bax to tBid, insertion of Bax into the MOM, Bax oligomerization, and finally permeabilization of the MOM (Lovell et al., 2008). Given that MSN-125, MSN-50, and DAN004 inhibit both cBid- and Bim-mediated activation of Bax the most likely explanation for inhibition of MOMP by the small molecules is direct binding to Bax. However, it was not possible to measure direct binding of MSN-50 or MSN-125 to Bax by isothermal calorimetry or nuclear magnetic resonance due to the limited solubility of the compounds and protein when mixed in solutions containing more than 100 nM Bax as required for such studies.

Although a formal possibility, it is unlikely that inhibition of Bax was due to partitioning of the compounds into the liposome bilayer and thereby changing its physical properties, because adding the compounds to liposomes and then re-isolating the liposomes by gel filtration chromatography had no effect on Bax-mediated MP (Figure S3). Furthermore, many structurally similar compounds of equal or higher hydrophobicity had no detectable effect on inhibition of MP (Table S1). Finally, it is unlikely that inhibiting Bax and Bak by changing the lipid properties of subcellular or artificial mitochondria-like membranes as employed in our studies would function or be tolerated in the wide variety of systems reported here.

The molecular mechanism(s) by which the compounds inhibit Bax in membranes was investigated using fluorescence spectroscopic and chemical crosslinking approaches. Bax binding to membranes is the step immediately prior to oligomerization and is affected by all of the upstream steps. To measure Bax binding to membranes, the intensity increase that results when the environment-sensitive dye 7-nitrobenzene-2-oxa-1,3-diazol-4-yl-ethylenediamine (NBD) attached to Bax inserts into the bilayer was monitored (Lovell et al., 2008). Neither MSN-125 nor MSN-50 significantly decreased the rate or extent to which NBD-labeled Bax bound to membranes in response to cBid (Figure 4A). Furthermore, preincubation of Bax labeled with Alexa 568 with DAN004 did not inhibit Bax binding to membranes as measured by Förster resonance energy transfer (FRET) between the Alexa dye and liposomes labeled with the long-chain dialkylcarbocyanine (Figure S1G). Finally, preincubation of Bax or mitochondria with MSN-125 did not inhibit Bax binding to mitochondria measured by differential centrifugation (Figure S1H).

To measure Bax oligomerization by FRET, single-cysteine mutants of Bax were labeled with diaminomethyl-coumarin (DAC-Bax-134C) as donor and with NBD (NBD-Bax-126C) as acceptor (Lovell et al., 2008). In reactions containing liposomes and tBid, addition of MSN-125 or MSN-50 reduced FRET between DAC-Bax-134C and NBD-Bax-126C (Figure 4B), demonstrating that both compounds inhibit Bax oligomerization.

However, FRET measurements do not distinguish between inhibition of dimer or oligomer formation. Therefore, the oligomerization state was further assessed by chemical crosslinking of purified Bax. Using the amine-specific crosslinker disuccinimidyl suberate (DSS), we clearly demonstrate that MSN-50, MSN-125, and DAN004 inhibit tBid-induced Bax oligomerization in liposomes with a more pronounced effect on inhibiting the formation of higher-order oligomers than dimers (Figures 4C–4H). At the highest concentration tested, MSN-125 also inhibited Bax dimerization to a limited extent, an effect not seen for MSN-50. High concentrations of MSN-50, MSN-125, or DAN004 inhibited large oligomers of Bax to a similar extent as the positive control Bcl-XL (Figures 4C–4H). Shorter exposures of the immunoblots indicated that changes in the oligomer bands were not due to inhibition of Bax binding to membranes leading to decreases in the amount of monomer at higher concentrations of the inhibitors. As expected (Dewson et al., 2012), crosslinking with DSS also

Figure 4. MSN-125 Restricts Bax Oligomerization beyond Dimer Formation

- (A) MSN-125 and MSN-50 (10 μ M) did not inhibit tBid-activated Bax binding to liposomes. MSN-125, MSN-50 (10 μ M), or DMSO (as a control) was added to liposome incubations containing NBD-Bax-126C (100 nM) and tBid (20 nM). The time-dependent increase in fluorescence from NBD indicates Bax binding to liposomes. One representative measurement from three independent experiments is shown. See also Figures S1G, S1H, and S3.
- (B) MSN-125 and MSN-50 (10 μ M) reduced DAC-Bax-134C (20 nM) binding to NBD-Bax-126C (100 nM) on liposomes. F_0 indicates DAC-Bax-134C fluorescence before addition of NBD-Bax-126C. Binding of the proteins resulted in a time-dependent decrease in DAC-Bax-134C fluorescence (F) due to FRET between DAC and NBD. Addition of MSN-125 or MSN-50 decreased FRET compared with no compound control (Ctrl). One representative measurement from three independent experiments is shown.
- (C) MSN-125 blocks tBid-induced Bax oligomerization in liposomes. Bax oligomers were detected after chemical crosslinking with DSS by immunoblotting for Bax. Bax monomers, ~20 kDa. The shorter exposure of the monomer fraction shown below the panel indicates that the changes in crosslinked species (dimers, solid dot; larger oligomers, brackets) are not due to differences in the amount of Bax monomer in each lane. MW, molecular weight marker (kDa). One representative immunoblot of $n \geq 3$ is shown.
- (D) MSN-125 preferentially inhibits higher-order oligomerization of Bax. Quantification of crosslinking data from (C). Mean \pm SD for $n \geq 3$. * $p < 0.05$, ** $p < 0.01$, *** $p < 0.001$; one-way ANOVA, post hoc, Dunnett.
- (E–H) MSN-50 and DAN004 disrupt Bax oligomerization. Chemical crosslinking of Bax oligomers assayed as described in (C and D). (E and G) One representative immunoblot of $n = 3$ is shown. (F and H) Quantified immunoblot band intensities for three independent replicates.

generated intramolecular crosslinks resulting in faster migration and band smearing for the monomer species (**Figures 4C, 4E, and 4G**).

MSN-125 Inhibits Bax Oligomerization at Defined Dimer Interfaces

Previous disulfide crosslinking studies identified three dimer interfaces in Bax oligomers bound to mitochondria (Dewson et al., 2012; Zhang et al., 2010, 2016). Binding of the BH3 region of one Bax to the canonical BH1-3-groove of another Bax forms a BH3-groove interface, and is followed by binding of the two helices 6 and 9 in the neighboring Bax molecules that form the other two interfaces.

To determine whether MSN-125 inhibits the formation of a specific dimer interface in Bax oligomers, site-specific disulfide crosslinking was used. To this end, single- and double-cysteine Bax mutants predicted or previously shown to form disulfide-linked Bax homodimers when activated by an exogenous Bax BH3-peptide were targeted to mitochondria lacking Bax and Bak (Zhang et al., 2016) in the absence or presence of MSN-125. The resulting mitochondria-bound mutants were oxidized after incubation with mitochondria to induce disulfide crosslinking in the absence or presence of MSN-125. In the absence of MSN-125, single-cysteine Bax-E146C (mutation in helix 6) or Bax-A183C (mutation in helix 9) formed a disulfide-linked homodimer (**Figure 5A**, lanes 16/18, arrow). **Addition of MSN-125 inhibited formation of both dimer interfaces** (**Figure 5A**, lanes 14 and 20).

Quantification of the bands revealed that even though targeting of WT Bax (**Figure S1H**) and most of the Bax mutants to membranes is not affected by the inhibitors, targeting of some mutants was affected by the cysteine substitutions. Therefore, to quantify the effect of the compounds on crosslinking and correct for differences in the efficiencies of targeting of the various mutants to membranes, the mean fraction of dimer without inhibitor was set to one for each crosslinking pair (dash between circles) and compared with the fraction of dimer in the presence of inhibitor (dash between squares). Individual data points (circles and squares) were plotted to illustrate the spread in the data between independent replicates (**Figure 5B**).

To examine the BH3/helix 2 region binding to the canonical groove, two pairs of Bax mutants with single cysteines in the BH3/helix 2 region (Bax-L59C, Bax-T56C) and in the canonical groove (Bax-M79C in helix 3, Bax-R94C in helix 4) were analyzed. These mutants also generated disulfide-linked dimers (**Figure 5A**, lanes 2 and 6) that were inhibited by MSN-125 (**Figure 5A**, lanes 1–8). However, when two cysteines were included in this region of Bax (L59C/L76C) or in an adjacent area (L59C/M79C) the crosslinks were not inhibited by MSN-125 (**Figure 5A**, lanes 25–32), suggesting that **this part of the BH3-groove dimer interface** (**Figure 6**) is only partially blocked by the compound.

Consistent with this result, another pair of Bax mutants with single cysteines in the BH3 region/helix 2 (Bax-L63C) and in the groove/helix 5 (Bax-A112C) resulted in disulfide crosslinking that was not inhibited by MSN-125 (**Figure 5A**, compare lanes 10 to 12, and **Figure 5B**). Because the residues are positioned where the crosslinking was relatively weak the experiment was repeated with a fully coupled in vitro transcription/translation (TNT) system to produce more Bax-L63C and Bax-A112C pro-

tein (L63C + A112C) and confirmed that this crosslink is not inhibited by MSN-125 (**Figure 5A**, lanes 21–24, and 5B). Similar crosslinking results for the different Bax mutants were also obtained using MSN-50 (**Figure S4**), confirming that both MSN compounds inhibit some but not all Bax dimer interfaces.

To determine whether the inhibitors had a similar activity on Bak, crosslinking was performed for three previously known sites of interaction in Bak including the BH3-groove, helix 9, and the region upstream of helix 9 (Dewson et al., 2008; Iyer et al., 2015). As expected all of these crosslinks were inhibited by MSN-50 (**Figure 5A**, lanes 33–44, and 5B). Thus, correct formation of dimers is inhibited for both Bax and Bak by MSN-125 and MSN-50.

A schematic of the MSN-125-affected and -unaffected interaction sites in the BH3-groove interface is shown in **Figure 6**. These results suggest that when helix α 2 of one Bax binds to the canonical groove of another Bax, MSN-125 blocks the binding of the N-terminal helical turn of α 2 binding (T56), partially inhibits the binding of the next helical turn (L59), but does not affect binding of the third helical turn (L63) to the groove. Taken together, these results suggest that, although Bax and Bak homodimers form (**Figures 4** and **5**), the known dimer interfaces are at least partially disrupted by the MSN compounds (**Figure 6**).

As expected from our previous data suggesting that Bax oligomerization occurs after binding to membranes (Annis et al., 2005), cBid-mediated targeting of the WT and mutant Bax proteins to mitochondria in the crosslinking reactions was largely unaffected by MSN-125 (**Figures S1H** and **5A**, open circles). Therefore, MSN-125 does not significantly interfere with targeting of Bax monomers to mitochondria, but rather inhibits assembly of Bax oligomers at the MOM by interfering with multiple, yet not all, Bax-Bax interactions at the three dimer interfaces of Bax. MSN-125, MSN-50, and DAN004 prevent Bax oligomerization predominantly beyond the formation of dimers, suggesting that correct formation of the dimer is required for oligomerization. Our data also support the notion that, even after activation by a BH3-protein, **correct formation of Bax dimers and likely larger oligomers** (Uren et al., 2017) is essential to execute MOMP.

DISCUSSION

Here, we have discovered novel small-molecule inhibitors of both pro-apoptotic Bax and Bak. Using these compounds, we provide new insight into unresolved questions in the regulation of the molecular mechanism of Bax/Bak oligomerization in the MOM. We establish that neither the Bax/Bak monomer nor an imperfect dimer is sufficient to permeabilize membranes. Our results clearly show that Bax binding to membranes does not result in MP unless the protein oligomerizes. Furthermore, we demonstrate that pharmacological inhibition of Bax and Bak protects cells from undergoing apoptosis after a variety of stimuli.

In most cell types, Bax and Bak can functionally substitute for each other (Degenhardt et al., 2002; Mikhailov et al., 2003). Therefore, to inhibit apoptosis in cells by blocking MOMP it is essential to inhibit both proteins. Unlike previously characterized molecules that inhibited Bax (Bombrun et al., 2003; Hetz et al., 2005; Peixoto et al., 2009; Polster et al., 2003), MSN-50, MSN-125, and DAN004 inhibit both Bax and Bak after activation by either cBid or Bim (**Figure 2**) protecting cells expressing either

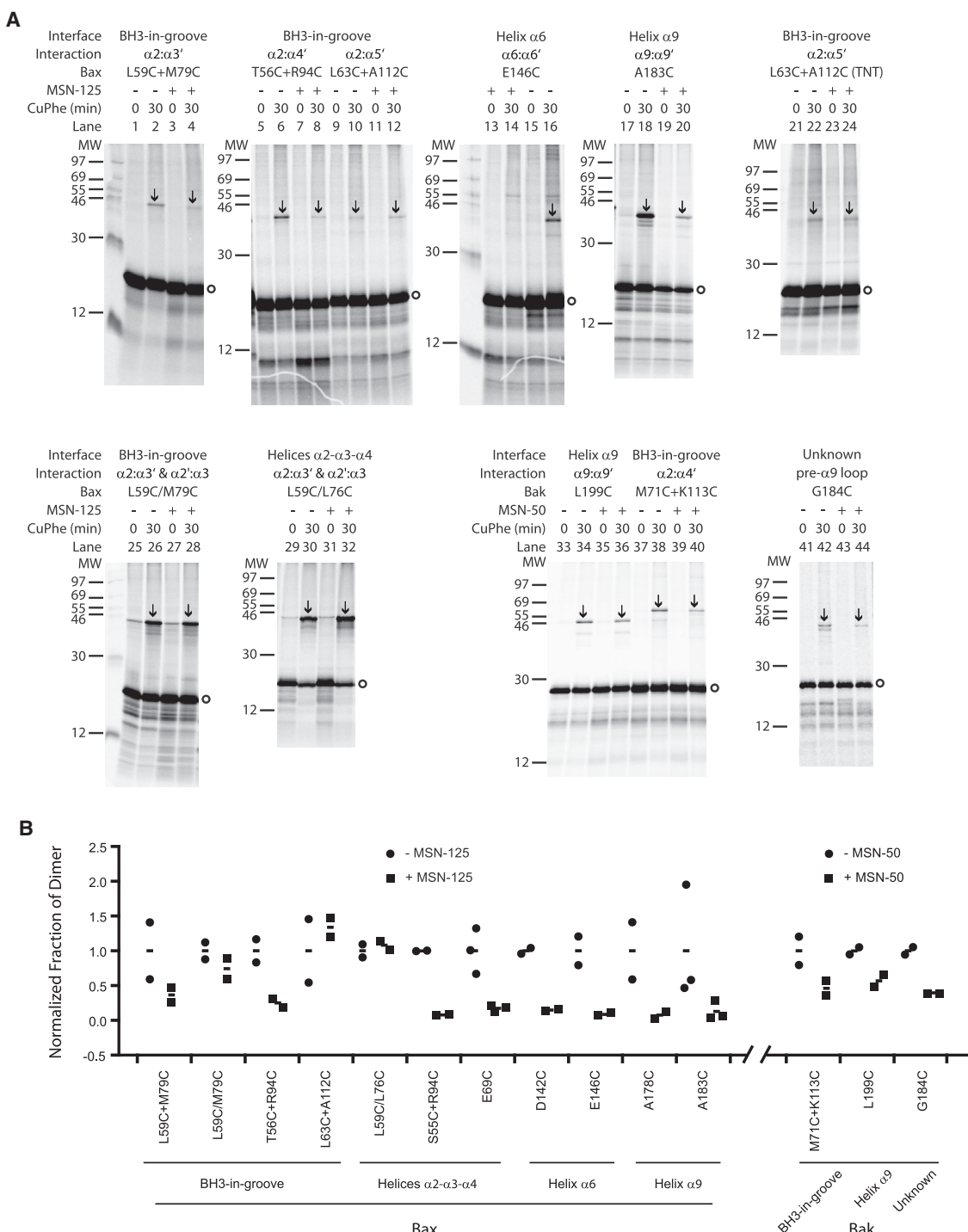
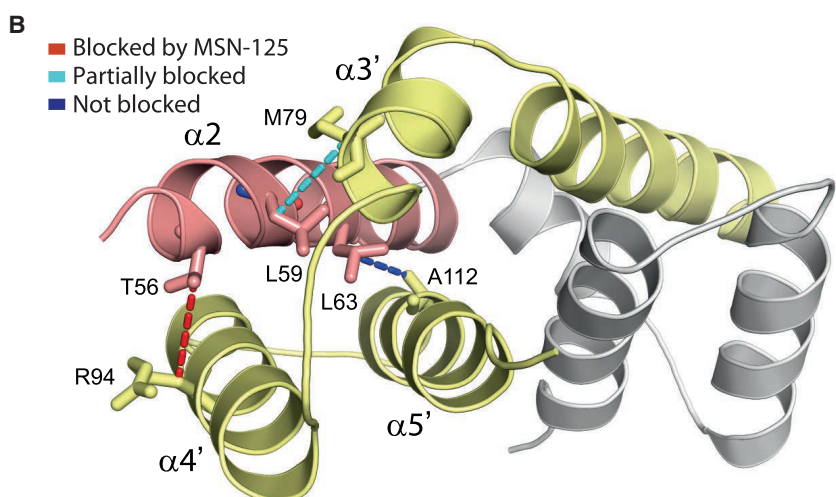
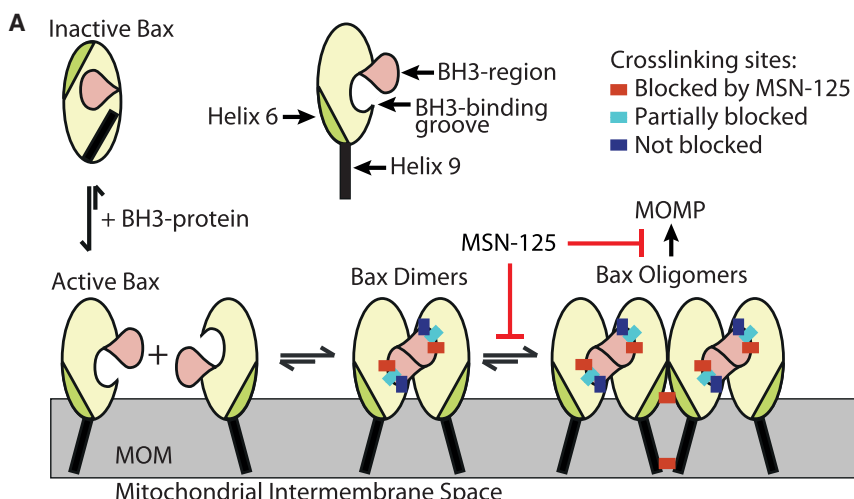


Figure 5. MSN-125 and MSN-50 Inhibit Some, but Not All, Interactions in Bax and Bak Dimers

(A) Autoradiography of disulfide crosslinking of single- or double-cysteine Bax or Bak incubated with mitochondria lacking Bax and Bak in the absence or presence of MSN-125 or MSN-50 (40 μ M) as indicated above the panels. MW, molecular weight marker (kDa); Bax monomers, circles; disulfide-linked Bax dimers, arrows. Addition of copper (II) (1,10-phenanthroline)₃ (CuPhe) oxidant for 30 min to induce disulfide crosslinking is indicated (min). Representative data from $n \geq 2$ experiments are shown.

(B) MSN-125 does not completely block the Bax dimer interface. Quantification of data from two to three independent experiments demonstrates that disulfide crosslinking of the single-cysteine Bax mutants L63C + A112C and the double-cysteine mutants L59C/L76C and L59/M79C were not inhibited by MSN-125. Quantification of all crosslinking pairs assayed as described in (A) are shown as individual data points (circles and squares) and means (dash). The single-cysteine Bax mutants L63C + A112C (TNT) were synthesized in the TNT system to increase protein yield and reduce the impact of background. Inhibition of crosslinking for similar interfaces in Bax by MSN-50 is shown in Figure S4.



Bax or Bak (Figure 3) from ActD and STS by preventing oligomerization of Bax and Bak (Figures 4, 5, and S4).

These small molecules inhibit permeabilization of the MOM by altering the BH3-groove dimer interface of Bax and Bak (Figures 5, 6, and S4). We speculate that partial disruption of this interface prevents the formation of the other interfaces required to form higher-order oligomers. Furthermore, we show that inhibition of oligomerization of both Bax and Bak is necessary and sufficient to inhibit genotoxic stress and broad kinase inhibition (STS)-induced apoptosis such that at least a subset of drug-treated cells retained proliferative potential (Figures 3A–3D).

Our cellular studies using MSN-50 and MSN-125 indicate that it might be possible to exploit inhibition of Bax and Bak therapeutically. Neuronal cell death after excitotoxicity has been demonstrated to be at least in part mediated through Bax-dependent signaling mechanisms (D'Orsi et al., 2012). Excitotoxicity is one of the damaging mechanisms contributing to acute neuronal degeneration after stroke (Mergenthaler et al., 2004), traumatic brain injury, and epileptic seizures (Engel et al., 2011). Genetic models where deletion of Bax protected neurons from cell death after stroke in mice (D'Orsi et al., 2015) further support the notion

Figure 6. MSN-125 and MSN-50 Interferes with Correct Dimer Formation for Bax and Bak thereby Inhibiting Further Oligomerization and Preventing MOMP

(A) Model of Bax oligomerization with schematic representation of the crosslinking positions (colored rectangles) that are not blocked (dark blue) or fully or partially blocked by MSN-125 (red and cyan, respectively); MOMP, mitochondrial outer membrane. While the model depicts MSN-125 and Bax it is representative of the data for both MSN-125 and MSN-50 as well as both Bax and Bak. (B) Schematic representation of the mechanism of MSN-125. Cartoon representation of the Bax BH3-groove dimer structure (PDB: 4BDU) shown with the BH3- $\alpha 2$ helix (pink) of one monomer (the rest of this monomer is colored gray) binding to the groove formed by $\alpha 3'$, $\alpha 4'$, and $\alpha 5'$ helices (yellow) of the other monomer. Disulfide crosslinking pairs are joined by dotted lines. Crosslinks blocked by MSN-125 (red), partially blocked (cyan), not blocked (blue) by MSN-125.

that inhibition of both Bax and Bak may be of therapeutic potential in acute neurodegeneration. Our data demonstrating that MSN-125 protects neurons from cell death after glutamate excitotoxicity (Figure 3E) establishes that pharmacological inhibition of Bax and Bak in neurons is feasible and may indeed provide therapeutic benefit. However, off-target effects with these tool compounds may contribute to the morphological alterations observed, and the high concentrations required limit the use of these compounds to *in vitro* investigations only.

Evidence of the function of Bak in neuronal apoptosis has been controversial. Bak may promote neuronal survival under certain conditions and in development, while promoting neuronal cell death after stress such as in stroke (Fanjiang et al., 2003; Hardwick and Soane, 2013). In addition, although full-length Bak is ubiquitously expressed in most cells, including central and peripheral nervous system neurons (Putcha et al., 2002; Sun et al., 2001), a neuron-specific splice variant of Bak, N-Bak, has been reported to have both anti- and pro-death functions (Sun et al., 2001; Uo et al., 2005). While evidence for the existence of this splice variant on the protein and functional level is inconclusive (Jakobson et al., 2012; Putcha et al., 2002), the inhibitors we have developed here offer the opportunity to investigate the role of Bax and Bak in the execution of MOMP in neurons and their role in the molecular pathophysiology of diseases of the nervous system.

To permeabilize membranes, Bax and Bak first homodimerize via the BH3-groove interface leading to the formation of heterogeneously sized higher-order oligomers via additional dimer interfaces (Czabotar et al., 2013; Dewson et al., 2012; Iyer et al., 2015; Ma et al., 2013; Subburaj et al., 2015). Which of these species permeabilizes the membrane is controversial with recent evidence suggesting that relatively disordered oligomers of

dimers are sufficient to permeabilize membranes (Uren et al., 2017). We have recently shown that the BH3-groove dimer nucleates the assembly of the Bax oligomeric pore, which is enlarged by dimerization at the helix 9 interface (Liao et al., 2016; Zhang et al., 2016). Using MSN-125 as a tool to dissect the molecular mechanism of Bax activation, we now show that blocking Bax at the dimer stage is sufficient to inhibit MOMP. Therefore, in contrast to results obtained with belted lipid nanodisks or MOM vesicles (Kushnareva et al., 2012; Xu et al., 2013) the minimal permeabilizing unit is a correctly formed dimer.

Crosslinking analysis revealed that MSN-125 disrupts helix 6 and helix 9 interactions, and some, but not all, interactions in the BH3-groove interface (Figures 5 and 6), suggesting that these interactions are necessary for Bax oligomerization. Consistent with this interpretation, the altered dimeric Bax structure is not recognized by the conformation-specific antibody 6A7 (Figure 3D). Therefore MSN-50 and MSN-125 can serve as important tools for identifying molecular interactions critical for forming functional Bax oligomers (Subburaj et al., 2015; Uren et al., 2017). We anticipate that these small molecules will allow further insight into the mechanism regulating formation, oligomerization, and the functional role of recently identified diverse oligomeric Bax-structures in forming an ordered “apoptotic pore” complex in the MOM (Grosse et al., 2016; Salvador-Gallego et al., 2016). Because MSN-125 inhibition of dimer interfaces is a downstream event and it inhibits heat-activated Bax (Figure S1I), we predict that the compounds will inhibit apoptosis induced by small molecules (Brahmbhatt et al., 2016) or p53 in addition to pro-apoptotic BH3-proteins (Follis et al., 2015).

In essence, three classes of functional Bax inhibitors have been reported (Bombrun et al., 2003; Hetz et al., 2005; Jiang et al., 2007; Peixoto et al., 2009, 2015; Polster et al., 2003), at least one class is sufficiently hydrophobic that it is expected to partition into membranes (Polster et al., 2003). Bax and Bak have to insert into and permeabilize membranes to lead to MOMP. Therefore, it is not surprising that other small molecules that alter the physical properties of membranes such as dibucaine, propranolol, and cholesterol have all been shown to partially inhibit the insertion of Bax into membranes, thereby reducing apoptosis (Christenson et al., 2008; Polster et al., 2003). However, gross perturbation of cellular membranes is expected to have wide-ranging effects on cellular physiology that are likely independent of a Bax/Bak-mediated pathway.

While access to some of the other molecules has been limited, it has been shown that most of them inhibit Bax, and they either do not inhibit Bak or the effect on Bak activity remains to be determined (Hetz et al., 2005). Furthermore, electrophysiology studies suggested that they act as channel blockers rather than inhibiting Bax oligomerization in the MOM or inhibiting Bak (Bombrun et al., 2003; Hetz et al., 2005; Peixoto et al., 2009; Polster et al., 2003). Using fluorescence spectroscopy and biochemical crosslinking, we show that MSN-50 and MSN-125 directly disrupt the correct formation of dimers and higher-order Bax oligomers, suggesting that they do not act as channel blockers.

The sole member of the third class, the MDM2 inhibitor Nutlin-3a, which we used as a control, has been reported to inhibit Bax and Bak oligomerization as an off-target effect, in addition to its intended inhibitory effect on the interaction of MDM2 and

p53 (Jiang et al., 2007). Assessment of the molecular mechanism of inhibiting Bax and Bak by Nutlin-3a suggests it inhibits Bax dimerization (Jiang et al., 2007), indicating a different and uncharacterized molecular mechanism from the molecules described here that allow dimer formation but alter the interfaces. Moreover, it remains unclear how Nutlins confer protective effects in kidney tubular cells but also potentiate cancer cell death (Tovar et al., 2006). Finally, Nutlin-3a is much less potent in inhibiting MOMP than MSN-50 and MSN-125 (Figure S1B).

In aggregate our results demonstrate that small-molecule inhibition of Bax and Bak oligomerization via partial disruption of the canonical BH3 peptide-groove interface prevents cells from executing MOMP in response to diverse apoptotic stimuli. Our studies not only provide novel insight into the mechanism of Bax oligomerization in the MOM, but also provide crucial tools for future mechanistic studies of the molecular organization of Bax and Bak oligomeric structures in the MOM. These tool compounds may also facilitate the development of future compounds designed to inhibit apoptosis by restricting MOMP in a wide range of diseases, including acute neurodegeneration, or for mitigating dose-limiting side effects of some cancer treatments.

SIGNIFICANCE

Mitochondrial outer membrane permeabilization and subsequent cell death underlies several degenerative diseases including acute neurodegeneration in stroke and can be an undesired side effect of cancer therapy in normal tissues. MOMP is executed by the pro-apoptotic Bcl-2 protein family members Bax and Bak in the MOM, and is an irreversible step in committing a cell to die. We report the discovery of small-molecule inhibitors of both Bax and Bak oligomerization that promote cell survival after apoptotic stimuli and protect primary neurons from death after excitotoxicity. We demonstrate that these compounds prevent Bax and Bak oligomerization by partially disrupting the canonical BH3 peptide-groove interface and preventing interactions at subsequent interfaces and thereby establish that neither the Bax/Bak monomer nor the partially defective dimer is sufficient to permeabilize membranes and thus to execute MOMP. Our work thus provides novel insight into the Bax/Bak-mediated regulation of MOMP as well as novel tools to dissect the mechanisms of Bax/Bak oligomerization leading to MOMP.

STAR★METHODS

Detailed methods are provided in the online version of this paper and include the following:

- KEY RESOURCES TABLE
- CONTACT FOR REAGENT AND RESOURCE SHARING
- EXPERIMENTAL MODEL AND SUBJECT DETAILS
- METHOD DETAILS
 - Protein Purification
 - Liposome Permeabilization and Dye Release Assays
 - Small Molecule Bax Inhibitor Screen

- Compounds and Synthesis
- Mitochondria Isolation and Permeabilization Assay
- Long Term Survival after Replating
- Immunofluorescence
- Primary Neuronal Cultures
- Bax:Bax Bax:Membrane FRET Assay
- Disuccinimidyl Suberate (DSS) Crosslinking
- Disulfide Crosslinking
- QUANTIFICATION AND STATISTICAL ANALYSIS

SUPPLEMENTAL INFORMATION

Supplemental Information includes four figures, one table, and supplemental text and can be found with this article online at <http://dx.doi.org/10.1016/j.chembiol.2017.03.011>.

AUTHOR CONTRIBUTIONS

J.Y. and D.W.A. designed and X.N. conducted the secondary screen with the 38 compounds, measured the IC₅₀ values for MSN-50, MSN-125, BJ-1, and BJ-1-BP, performed the immunofluorescence 6A7 experiments, and conducted the Bax-Bax FRET experiments. H.B. tested the activity of DAN004 in the liposome-based assay and in the HCT116 cells, examined the efficacy of all the compounds in the mitochondria-based assay, conducted the DSS crosslinking studies, compared inhibition of cBid/Bim-Bax by the compounds, and conducted the isothermal calorimetry studies with Bax. P.M. designed the assay and tested the activity of MSN-125 in primary neurons. J.L. designed and Z.Z. conducted the mitochondrial binding and disulfide crosslinking studies with Bax and Bak. J.S. conducted the SAR studies in the liposome-based assay shown in Table S1. W.E.D., C.C., and D.W.A. designed DAN004. W.E.D. designed the synthetic strategy, M.D. and F.G.R.E. synthesized DAN004. C.C. designed and performed preliminary tests on the compound. E.W. conducted the primary screen with 86 compounds. W.Z. conducted the clonal survival assays in the HCT116 cells, J.P. conducted experiments with Nutlin-3a and DAN004. P.A. designed and J.N., M.S., and R.J. synthesized MSN-50, MSN-125, and the SAR compounds. D.W.A., B.L., and J.Y. conceived and directed the project. X.N., H.B., P.M., B.L., and D.W.A. analyzed the data and wrote the paper.

ACKNOWLEDGMENTS

We thank M. Falcone for conducting the compound partitioning experiments and C. Griffiths for assistance in the screen. This work was supported by the Ontario Institute for Cancer Research through funding provided by the Government of Ontario, the Terry Fox Research Institute, the W. Garfield Weston Foundation – Brain Canada Foundation Multi-Investigator Research Initiative (MIRI), and Canadian Institutes of Health Research, Foundation Grant FDN143312 (D.W.A.), the National Cancer Institute of Canada and Department of Science and Technology (P.A.), the Shanghai Municipal Science and Technology Commission 10410704000 (J.Y. and D.W.A.), the Shanghai Municipal Education Commission J50201 (J.Y.), the European Union's Seventh Framework Program (FP7/2008–2013) under Grant Agreement 627951 (Marie Curie IOF to P.M.), and the German Academic Exchange Service DAAD PPP Canada program with funds of the German Federal Ministry of Education and Research (grant 57212163 to P.M.), and the United States NIH grant GM062964 and the Oklahoma Center for the Advancement of Science and Technology grant HR16-026, and a Presbyterian Health Foundation seed grant GRF00000125 (J.L.). D.W.A. is a Tier 1 Canada Research Chair. P.M. is a fellow of the BIH Charité Clinician Scientist Program funded by the Charité Universitätsmedizin Berlin and the Berlin Institute of Health, and R.J. received a PhD fellowship from the Council of Scientific and Industrial Research.

Received: August 12, 2016

Revised: December 29, 2016

Accepted: March 13, 2017

Published: April 6, 2017

REFERENCES

- Andrews, D.W. (2014). Pores of no return. *Mol. Cell* 56, 465–466.
- Annis, M.G., Soucie, E.L., Dlugosz, P.J., Cruz-Aguado, J.A., Penn, L.Z., Leber, B., and Andrews, D.W. (2005). Bax forms multispanning monomers that oligomerize to permeabilize membranes during apoptosis. *EMBO J.* 24, 2096–2103.
- Bilien, L.P., Kokoski, C.L., Lovell, J.F., Leber, B., and Andrews, D.W. (2008). Bcl-XL inhibits membrane permeabilization by competing with Bax. *PLoS Biol.* 6, e147.
- Bogner, C., Leber, B., and Andrews, D.W. (2010). Apoptosis: embedded in membranes. *Curr. Opin. Cell Biol.* 22, 845–851.
- Bombrun, A., Gerber, P., Casi, G., Terradillos, O., Antonsson, B., and Halazy, S. (2003). 3,6-Dibromocarbazole piperazine derivatives of 2-propanol as first inhibitors of cytochrome c release via Bax channel modulation. *J. Med. Chem.* 46, 4365–4368.
- Brahmbhatt, H., Uehling, D., Al-Awar, R., Leber, B., and Andrews, D. (2016). Small molecules reveal an alternative mechanism of Bax activation. *Biochem. J.* 473, 1073–1083.
- Christenson, E., Merlin, S., Saito, M., and Schlesinger, P. (2008). Cholesterol effects on BAX pore activation. *J. Mol. Biol.* 381, 1168–1183.
- Czabotar, P.E., Westphal, D., Dewson, G., Ma, S., Hockings, C., Fairlie, W.D., Lee, E.F., Yao, S., Robin, A.Y., Smith, B.J., et al. (2013). Bax crystal structures reveal how BH3 domains activate Bax and nucleate its oligomerization to induce apoptosis. *Cell* 152, 519–531.
- D'Orsi, B., Bonner, H., Tuffy, L.P., Dussmann, H., Woods, I., Courtney, M.J., Ward, M.W., and Prehn, J.H. (2012). Calpains are downstream effectors of bax-dependent excitotoxic apoptosis. *J. Neurosci.* 32, 1847–1858.
- D'Orsi, B., Kilbride, S.M., Chen, G., Perez Alvarez, S., Bonner, H.P., Pfeiffer, S., Plesnila, N., Engel, T., Henshall, D.C., Dussmann, H., et al. (2015). Bax regulates neuronal Ca²⁺ homeostasis. *J. Neurosci.* 35, 1706–1722.
- Danial, N.N., and Korsmeyer, S.J. (2004). Cell death: critical control points. *Cell* 116, 205–219.
- Degenhardt, K., Sundararajan, R., Lindsten, T., Thompson, C., and White, E. (2002). Bax and Bak independently promote cytochrome C release from mitochondria. *J. Biol. Chem.* 277, 14127–14134.
- Delbridge, A.R., Valente, L.J., and Strasser, A. (2012). The role of the apoptotic machinery in tumor suppression. *Cold Spring Harb Perspect. Biol.* 4, <http://dx.doi.org/10.1101/cshperspect.a008789>.
- Dewson, G., Kratina, T., Sim, H.W., Puthalakath, H., Adams, J.M., Colman, P.M., and Kluck, R.M. (2008). To trigger apoptosis, Bak exposes its BH3 domain and homodimerizes via BH3:groove interactions. *Mol. Cell* 30, 369–380.
- Dewson, G., Ma, S., Frederick, P., Hockings, C., Tan, I., Kratina, T., and Kluck, R.M. (2012). Bax dimerizes via a symmetric BH3:groove interface during apoptosis. *Cell Death Differ.* 19, 661–670.
- Engel, T., Plesnila, N., Prehn, J.H., and Henshall, D.C. (2011). In vivo contributions of BH3-only proteins to neuronal death following seizures, ischemia, and traumatic brain injury. *J. Cereb. Blood Flow Metab.* 31, 1196–1210.
- Fannjiang, Y., Kim, C.H., Huganir, R.L., Zou, S., Lindsten, T., Thompson, C.B., Mito, T., Traystman, R.J., Larsen, T., Griffin, D.E., et al. (2003). BAK alters neuronal excitability and can switch from anti- to pro-death function during postnatal development. *Dev. Cell* 4, 575–585.
- Follis, A.V., Llambi, F., Merritt, P., Chipuk, J.E., Green, D.R., and Kriwacki, R.W. (2015). Pin1-induced proline isomerization in cytosolic p53 mediates BAX activation and apoptosis. *Mol. Cell* 59, 677–684.
- Grosje, L., Wurm, C.A., Bruser, C., Neumann, D., Jans, D.C., and Jakobs, S. (2016). Bax assembles into large ring-like structures remodeling the mitochondrial outer membrane in apoptosis. *EMBO J.* 35, 402–413.
- Hardwick, J.M., and Soane, L. (2013). Multiple functions of BCL-2 family proteins. *Cold Spring Harb Perspect. Biol.* 5, <http://dx.doi.org/10.1101/cshperspect.a008722>.
- Hetz, C., Vitte, P.A., Bombrun, A., Rostovtseva, T.K., Montessuit, S., Hiver, A., Schwarz, M.K., Church, D.J., Korsmeyer, S.J., Martinou, J.C., et al. (2005). Bax

- channel inhibitors prevent mitochondrion-mediated apoptosis and protect neurons in a model of global brain ischemia. *J. Biol. Chem.* **280**, 42960–42970.
- Hsu, Y.T., and Youle, R.J. (1997). Nonionic detergents induce dimerization among members of the Bcl-2 family. *J. Biol. Chem.* **272**, 13829–13834.
- Hsu, Y.T., and Youle, R.J. (1998). Bax in murine thymus is a soluble monomeric protein that displays differential detergent-induced conformations. *J. Biol. Chem.* **273**, 10777–10783.
- Iyer, S., Bell, F., Westphal, D., Anwari, K., Gulbis, J., Smith, B.J., Dewson, G., and Kluck, R.M. (2015). Bak apoptotic pores involve a flexible C-terminal region and juxtaposition of the C-terminal transmembrane domains. *Cell Death Differ.* **22**, 1665–1675.
- Jakobson, M., Lintulahti, A., and Arumae, U. (2012). mRNA for N-Bak, a neuron-specific BH3-only splice isoform of Bak, escapes nonsense-mediated decay and is translationally repressed in the neurons. *Cell Death Dis.* **3**, e269.
- Jiang, M., Pabla, N., Murphy, R.F., Yang, T., Yin, X.M., Degenhardt, K., White, E., and Dong, Z. (2007). Nutlin-3 protects kidney cells during cisplatin therapy by suppressing Bax/Bak activation. *J. Biol. Chem.* **282**, 2636–2645.
- Kushnareva, Y., Andreyev, A.Y., Kuwana, T., and Newmeyer, D.D. (2012). Bax activation initiates the assembly of a multimeric catalyst that facilitates Bak pore formation in mitochondrial outer membranes. *PLoS Biol.* **10**, e1001394.
- Leber, B., Geng, F., Kale, J., and Andrews, D.W. (2010). Drugs targeting Bcl-2 family members as an emerging strategy in cancer. *Expert Rev. Mol. Med.* **12**, e28.
- Liao, C., Zhang, Z., Kale, J., Andrews, D.W., Lin, J., and Li, J. (2016). Conformational heterogeneity of Bax helix 9 dimer for apoptotic pore formation. *Sci. Rep.* **6**, 29502.
- Lovell, J.F., Billen, L.P., Bindner, S., Shamas-Din, A., Fradin, C., Leber, B., and Andrews, D.W. (2008). Membrane binding by tBid initiates an ordered series of events culminating in membrane permeabilization by Bax. *Cell* **135**, 1074–1084.
- Ma, S., Hockings, C., Anwari, K., Kratina, T., Fennell, S., Lazarou, M., Ryan, M.T., Kluck, R.M., and Dewson, G. (2013). Assembly of the Bak apoptotic pore: a critical role for the Bak protein alpha6 helix in the multimerization of homodimers during apoptosis. *J. Biol. Chem.* **288**, 26027–26038.
- Mathew, R., Degenhardt, K., Haramaty, L., Karp, C.M., and White, E. (2008). Immortalized mouse epithelial cell models to study the role of apoptosis in cancer. *Methods Enzymol.* **446**, 77–106.
- Mergenthaler, P., Dirmagl, U., and Meisel, A. (2004). Pathophysiology of stroke: lessons from animal models. *Metab. Brain Dis.* **19**, 151–167.
- Mergenthaler, P., Kahl, A., Kamitz, A., van Laak, V., Stohlmann, K., Thomsen, S., Klawitter, H., Przesdzinski, I., Neeb, L., Freyer, D., et al. (2012). Mitochondrial hexokinase II (HKII) and phosphoprotein enriched in astrocytes (PEA15) form a molecular switch governing cellular fate depending on the metabolic state. *Proc. Natl. Acad. Sci. USA* **109**, 1518–1523.
- Mikhailov, V., Mikhailova, M., Degenhardt, K., Venkatachalam, M.A., White, E., and Saikumar, P. (2003). Association of Bax and Bak homo-oligomers in mitochondria. Bax requirement for Bak reorganization and cytochrome c release. *J. Biol. Chem.* **278**, 5367–5376.
- Moldoveanu, T., Follis, A.V., Kriwacki, R.W., and Green, D.R. (2014). Many players in BCL-2 family affairs. *Trends Biochem. Sci.* **39**, 101–111.
- Peixoto, P.M., Ryu, S.Y., Bombrun, A., Antonsson, B., and Kinnally, K.W. (2009). MAC inhibitors suppress mitochondrial apoptosis. *Biochem. J.* **423**, 381–387.
- Peixoto, P.M., Teijido, O., Mirzalieva, O., Dejean, L.M., Pavlov, E.V., Antonsson, B., and Kinnally, K.W. (2015). MAC inhibitors antagonize the pro-apoptotic effects of tBid and disassemble Bax/Bak oligomers. *J. Bioenerg. Biomembr.* **49**, 65–74.
- Polster, B.M., Basanez, G., Young, M., Suzuki, M., and Fiskum, G. (2003). Inhibition of Bax-induced cytochrome c release from neural cell and brain mitochondria by dibucaine and propranolol. *J. Neurosci.* **23**, 2735–2743.
- Prakesch, M., Denisov, A.Y., Naim, M., Gehring, K., and Arya, P. (2008). The discovery of small molecule chemical probes of Bcl-X(L) and Mcl-1. *Bioorg. Med. Chem.* **16**, 7443–7449.
- Putcha, G.V., Harris, C.A., Moulder, K.L., Easton, R.M., Thompson, C.B., and Johnson, E.M., Jr. (2002). Intrinsic and extrinsic pathway signaling during neuronal apoptosis: lessons from the analysis of mutant mice. *J. Cell Biol.* **157**, 441–453.
- Salvador-Gallego, R., Mund, M., Cosentino, K., Schneider, J., Unsay, J., Schraermeyer, U., Engelhardt, J., Ries, J., and Garcia-Saez, A.J. (2016). Bax assembly into rings and arcs in apoptotic mitochondria is linked to membrane pores. *EMBO J.* **35**, 389–401.
- Sarosiek, K.A., Chi, X., Bachman, J.A., Sims, J.J., Montero, J., Patel, L., Flanagan, A., Andrews, D.W., Sorger, P., and Letai, A. (2013). BID preferentially activates BAK while BIM preferentially activates BAX, affecting chemotherapy response. *Mol. Cell* **51**, 751–765.
- Satsoura, D., Kucerka, N., Shivakumar, S., Pencer, J., Griffiths, C., Leber, B., Andrews, D.W., Katsaras, J., and Fradin, C. (2012). Interaction of the full-length Bax protein with biomimetic mitochondrial liposomes: a small-angle neutron scattering and fluorescence study. *Biochim. Biophys. Acta* **1818**, 384–401.
- Shamas-Din, A., Bindner, S., Zhu, W., Zaltsman, Y., Campbell, C., Gross, A., Leber, B., Andrews, D.W., and Fradin, C. (2013). tBid undergoes multiple conformational changes at the membrane required for Bax activation. *J. Biol. Chem.* **288**, 22111–22127.
- Shamas-Din, A., Satsoura, D., Khan, O., Zhu, W., Leber, B., Fradin, C., and Andrews, D.W. (2014). Multiple partners can kiss-and-run: Bax transfers between multiple membranes and permeabilizes those primed by tBid. *Cell Death Dis.* **5**, e1277.
- Subburaj, Y., Cosentino, K., Axmann, M., Pedrueza-Villalmanzo, E., Hermann, E., Bleicken, S., Spatz, J., and Garcia-Saez, A.J. (2015). Bax monomers form dimer units in the membrane that further self-assemble into multiple oligomeric species. *Nat. Commun.* **6**, 8042.
- Sun, Y.F., Yu, L.Y., Saarma, M., Timmus, T., and Arumae, U. (2001). Neuron-specific Bcl-2 homology 3 domain-only splice variant of Bak is anti-apoptotic in neurons, but pro-apoptotic in non-neuronal cells. *J. Biol. Chem.* **276**, 16240–16247.
- Szeto, H.H. (2008). Mitochondria-targeted cytoprotective peptides for ischemia-reperfusion injury. *Antioxid. Redox Signal.* **10**, 601–619.
- Tan, C., Dlugosz, P.J., Peng, J., Zhang, Z., Lapolla, S.M., Plafker, S.M., Andrews, D.W., and Lin, J. (2006). Auto-activation of the apoptosis protein Bax increases mitochondrial membrane permeability and is inhibited by Bcl-2. *J. Biol. Chem.* **281**, 14764–14775.
- Tovar, C., Rosinski, J., Filipovic, Z., Higgins, B., Kolinsky, K., Hilton, H., Zhao, X., Vu, B.T., Qing, W., Packman, K., et al. (2006). Small-molecule MDM2 antagonists reveal aberrant p53 signaling in cancer: implications for therapy. *Proc. Natl. Acad. Sci. USA* **103**, 1888–1893.
- Uo, T., Kinoshita, Y., and Morrison, R.S. (2005). Neurons exclusively express N-Bak, a BH3 domain-only Bak isoform that promotes neuronal apoptosis. *J. Biol. Chem.* **280**, 9065–9073.
- Uren, R.T., O'Hely, M., Iyer, S., Bartolo, R., Shi, M.X., Brouwer, J.M., Alsop, A.E., Dewson, G., and Kluck, R.M. (2017). Disordered clusters of Bak dimers rupture mitochondria during apoptosis. *eLife* **6**, <http://dx.doi.org/10.7554/eLife.19944>.
- Wang, C., and Youle, R.J. (2012). Predominant requirement of Bax for apoptosis in HCT116 cells is determined by Mcl-1's inhibitory effect on Bak. *Oncogene* **31**, 3177–3189.
- Willis, S.N., Fletcher, J.I., Kaufmann, T., van Delft, M.F., Chen, L., Czabotar, P.E., Ierino, H., Lee, E.F., Fairlie, W.D., Bouillet, P., et al. (2007). Apoptosis initiated when BH3 ligands engage multiple Bcl-2 homologs, not Bax or Bak. *Science* **315**, 856–859.
- Wilson-Annan, J., O'Reilly, L.A., Crawford, S.A., Hausmann, G., Beaumont, J.G., Parma, L.P., Chen, L., Lackmann, M., Lithgow, T., Hinds, M.G., et al. (2003). Proapoptotic BH3-only proteins trigger membrane integration of pro-survival Bcl-w and neutralize its activity. *J. Cell Biol.* **162**, 877–887.

- Xu, X.P., Zhai, D., Kim, E., Swift, M., Reed, J.C., Volkmann, N., and Hanein, D. (2013). Three-dimensional structure of Bax-mediated pores in membrane bilayers. *Cell Death Dis.* 4, e683.
- Yamaguchi, R., Andreyev, A., Murphy, A.N., Perkins, G.A., Ellisman, M.H., and Newmeyer, D.D. (2007). Mitochondria frozen with trehalose retain a number of biological functions and preserve outer membrane integrity. *Cell Death Differ.* 14, 616–624.
- Zhang, Z., Zhu, W., Lapolla, S.M., Miao, Y., Shao, Y., Falcone, M., Boreham, D., McFarlane, N., Ding, J., Johnson, A.E., et al. (2010). Bax forms an oligomer via separate, yet interdependent, surfaces. *J. Biol. Chem.* 285, 17614–17627.
- Zhang, Z., Subramaniam, S., Kale, J., Liao, C., Huang, B., Brahmbhatt, H., Condon, S.G., Lapolla, S.M., Hays, F.A., Ding, J., et al. (2016). BH3-in-groove dimerization initiates and helix 9 dimerization expands Bax pore assembly in membranes. *EMBO J.* 35, 208–236.

STAR★METHODS

KEY RESOURCES TABLE

REAGENT or RESOURCE	SOURCE	IDENTIFIER
Antibodies		
Mouse monoclonal anti-Bax 6A7, 2D2	Laboratory of Dr. Richard Youle; Hsu and Youle, 1997	N/A
Sheep polyclonal anti-cytochrome c	Serum obtained from Capriologics; antibody purified in our laboratory	N/A
Donkey anti-sheep - Alexa Fluor 488	Invitrogen	Cat # A-11015
Goat anti-mouse- Alexa Fluor 555	Invitrogen	Cat # A-21422
Bacterial and Virus Strains		
Escherichia coli BL21-AI	New England Biolabs	Cat # C2528
Escherichia coli DH5 α	New England Biolabs	Cat # C2988J
Chemicals, Peptides, and Recombinant Proteins		
Nutlin-3a	Selleck	Cat # S8059; CAS: 675576-98-4
Actinomycin D	Sigma	Cat # A9415; CAS: 50-76-0
Staurosporine	Sigma	Cat # S5921; CAS: 62996-74-1
Disuccinimidyl suberate	Thermo Scientific Pierce	Cat # 21655; CAS: 68528-80-3
Crystal Violet	Sigma	Cat# HT901; CAS: 548-62-9
8-Aminonaphthalene-1,3,6-Trisulfonic Acid, Disodium Salt	Life Technologies	Cat # A350; CAS: 5398-34-5
p-Xylene-Bis-Pyridinium Bromide	Life Technologies	Cat # X1525; CAS: 14208-10-7
DAPI	Sigma	Cat # D9542; CAS: 28718-90-3
IANBD	Life Technologies	Cat # D2004; CAS: 173485-12-6
DACM	AnaSpec	Cat # AS-81403
Alexa Fluor 568	Life Technologies	Cat # A20341
DiD	Life Technologies	Cat # D7757
Caspase-8	Enzo Life Sciences	Cat # BML-SE172-5000
β -NADH	Sigma	Cat # N8129; CAS: 606-68-8
I-lactic dehydrogenase	Sigma	Cat # L3916; CAS: 9001-60-9
Experimental Models: Cell Lines		
Mouse: Baby mouse kidney cells	Laboratory of Dr. Eileen White; Mathew et al., 2008	N/A
Human: HCT116 cells	Wang and Youle, 2012	N/A
Experimental Models: Organisms/Strains		
Mouse: C57bl/6J. E15 embryos to generate primary embryonic mouse brain cortical neuronal culture	The Jackson Laboratory, continuous breeding in house	JAX: 000664
Mouse: B6.129-Bak1tm1Thsn/J	The Jackson Laboratory	JAX: 004183
Recombinant DNA		
pvitro1-blasti-smac-mCherry	Shamas-Din et al., 2014	N/A
Software and Algorithms		
GraphPad Prism	GraphPad Software, Inc.,	https://www.graphpad.com/
ImageJ	National Institutes of Health	https://imagej.nih.gov/ij/
SPSS	IBM	https://www.ibm.com/analytics/us/en/technology/spss/
Other		
TNT-coupled SP6 RNA polymerase/ reticulocyte lysate system	Promega	Cat # L4600
Cytochrome c ELISA	R&D systems	Cat # MCTC0

(Continued on next page)

Continued

REAGENT or RESOURCE	SOURCE	IDENTIFIER
L- α -phosphatidylcholine	Avanti Polar Lipids	Cat # 840051C
L- α -phosphatidylethanolamine	Avanti Polar Lipids	Cat # 841118C
L- α -phosphatidylinositol	Avanti Polar Lipids	Cat # 840042C
1,2-dioleoyl-sn-glycero-3-phospho-L-serine (sodium salt)	Avanti Polar Lipids	Cat # 840035C
1',3'-bis[1,2-dioleoyl-sn-glycero-3-phospho]-sn-glycerol (sodium salt)	Avanti Polar Lipids	Cat # 710335C

CONTACT FOR REAGENT AND RESOURCE SHARING

For reagents and resources other than MSN-50 and MSN-125 generated in this study or any other questions about the reagents please contact David W. Andrews (david.andrews@sri.utoronto.ca). For all questions and inquiries regarding BJ-1, BJ-1BP, MSN-50 and MSN-125 please contact Prabhat Arya (prabhata@drils.org) for questions and inquiries regarding DAN004 please contact Wibke Diederich (wibke.diederich@staff.uni-marburg.de).

EXPERIMENTAL MODEL AND SUBJECT DETAILS

See [Method Details](#) below for details on cell cultures and culture conditions.

METHOD DETAILS

Protein Purification

Bax

Recombinant full length human Bax fused to a C- terminus intein tag containing a chitin binding domain was expressed in *Escherichia coli* BL21-AI and purified as described previously ([Billen et al., 2008](#); [Lovell et al., 2008](#)). Briefly, cells were resuspended in lysis buffer (10 mM Hepes (pH 7.2), 100 mM NaCl, 0.2% CHAPS, 1 mM phenylmethylsulfonylfluoride (PMSF), 10 μ g/ml DNase and 1 X protease inhibitor cocktail) and lysed by mechanical disruption in a French press. Bax was purified by affinity chromatography with a chitin column. Chitin beads were incubated with the lysate containing Bax for 2 hours at 4°C and washed with wash buffer (10 mM Hepes (pH 7.2), 500 mM NaCl, 0.5% CHAPS). Release of Bax from the intein tag was conducted by incubation of the chitin column in cleavage buffer (10mM Hepes (pH 7.2), 200 mM NaCl, 0.2 mM EDTA, 0.1% CHAPS and 100 mM β -mercaptoethanol) for 24-48 hrs at 4°C. The eluate containing Bax was passed over a DEAE Sepharose column 2-3 X to remove nucleic acid contaminants, dialyzed in dialysis buffer (10 mM Hepes (pH 7), 200 mM NaCl, 0.2 mM EDTA, 10 % glycerol), and stored at -80°C.

Mutants of Bax with a single cysteine at position 126 or 134 intended for labelling with fluorescent dyes were purified as described above except Bax was released from the intein tag in buffer containing 100 mM hydroxylamine instead of β -mercaptoethanol to prevent leaving a free sulphydryl at the carboxyl-terminus. The concentration of Bax was determined spectrophotometrically at 280 nm using the molar extinction coefficient 37,000 M⁻¹cm⁻¹. For labeling, N-N'-dimethyl-N-(iodoacetyl)-N'-(7-nitrobenzene-2-oxa-1,3-diazol-4-yl)ethylenediamine (IANBD; Life Technologies), N-(7-dimethylamino-4-methylcoumarin-3-yl) maleimide (DACM; Anaspec), or Alexa 568 C5-maleimide (Alexa568; Life Technologies) were prepared in DMSO and the concentrations were determined after dilution in methanol by absorbance using the dye molar extinction coefficients 25,000 M⁻¹cm⁻¹ at 479 nm, 27,000 M⁻¹cm⁻¹ at 380 nm, or 106,000 M⁻¹cm⁻¹ at 575 nm, respectively. Bax was labeled by incubation of the protein with a 10 fold molar excess of dye in labeling buffer (10 mM HEPES pH 7, 0.2 M NaCl, 0.2 mM EDTA, 0.5% CHAPS w/v and 10% glycerol v/v) with rotation at room temperature for 2 hours in the dark. The reaction was quenched with 1 mM dithiothreitol. Free dye was removed from the sample by gel filtration chromatography (Sephadex G-25 Fine, GE Healthcare Life Sciences) in the labeling buffer without CHAPS.

Bcl-XL

Recombinant full length human Bcl-XL fused to a C- terminal intein tag was expressed in *Escherichia coli* DH5 α cells as described previously ([Billen et al., 2008](#)). Bcl-XL was purified by affinity chromatography similar to Bax except the lysis and wash buffer contained 20mM Tris (pH 8), 500 mM NaCl, 0.5 mM EDTA, 1 % CHAPS, 1 mM PMSF, 10 μ g/ml DNase and 1 X protease inhibitor cocktail and intein cleavage was conducted in cleavage buffer containing 20 mM Tris (pH 8), 200 mM NaCl, 20 % glycerol, 0.2 % CHAPS, 100 mM β -mercaptoethanol. The eluate containing Bcl-XL was further purified on a phenyl- Sepharose column by elution with cleavage buffer without any salt, dialyzed in dialysis buffer (Tris (pH 8), 20% glycerol) and stored at -80 °C.

Bid

Recombinant full length murine Bid fused to a N- terminal histidine tag was expressed in *Escherichia coli* BL21-AI and purified as described previously ([Shamas-Din et al., 2013](#)). Briefly cells were resuspended in lysis buffer (10 mM Hepes (pH 7), 100mM NaCl, 10 mM imidazole, 1mM PMSF, 10 μ g/ml DNase and 1 x protease inhibitor cocktail) and lysed using mechanical disruption. Nickel

beads were incubated with the lysate for 2 hours at 4°C and washed with wash buffer (10 mM HEPES (pH 7), 300 mM NaCl, 1 % CHAPS, 10 mM imidazole). Fractions containing Bid were eluted in elution buffer (10 mM HEPES (pH 7), 100 mM NaCl, 200 mM imidazole, 0.1 % CHAPS, 10% glycerol). cBid was obtained by incubating fractions containing Bid with caspase-8 (Enzo Life Sciences) at room temperature for ~36–40 hrs. tBid was isolated by affinity chromatography using nickel heads and elution in elution buffer containing 2% (w/v) octylglucoside. cBid and tBid fractions were dialyzed in dialysis buffer (10 mM HEPES (pH 7), 100 mM NaCl, 0.1 mM EDTA, 10% glycerol) and stored at -80°C.

Bim

Recombinant full length murine BimL fused to a N-terminal histidine tag was expressed in Escherichia coli BL21-AI and purified as described previously ([Sarosiek et al., 2013](#)). Cells were lysed by mechanical disruption in lysis buffer (20 mM Tris (pH 8), 20 mM NaCl, 1% CHAPS, 5 mM imidazole, 20% glycerol). The lysate was passed through a nickel column and the column was washed with wash buffer (20 mM Tris (pH 8), 50 mM NaCl, 0.5 % CHAPS, 10 mM imidazole, 20% glycerol). Fractions containing Bim were obtained by eluting with elution buffer (20 mM Hepes (pH 7.2), 10 mM NaCl, 0.3% CHAPS, 300 mM imidazole, 20% glycerol). The concentration of NaCl in the eluate was adjusted to 150 mM and applied to a high performance phenyl sepharose column pre-equilibrated with buffer (20 mM Hepes (pH 7.2), 100 mM NaCl, 0.3% CHAPS, 20% glycerol). Fractions containing Bim were eluted in the equilibration buffer lacking NaCl, dialyzed in dialysis buffer (10 mM Hepes (pH 7), 1 mM NaCl, 20% glycerol), and stored at -80°C.

Liposome Permeabilization and Dye Release Assays

Mitochondria-like liposomes (48% phosphatidylcholine, 28% phosphatidylethanolamine, 10% phosphatidylinositol, 10% dioleoyl phosphatidylserine and 4% tetraoleoyl cardiolipin (Avanti)) encapsulating aminonaphthalene1,3,6-trisulfonic acid (ANTS) and its quencher, 45 mM p-xylene-bis-pyridinium (DPX, Life Technologies) were prepared in buffer containing 10 mM HEPES (7.2), 200 mM potassium chloride, 5 mM magnesium chloride and 0.2 mM EDTA as described previously ([Billen et al., 2008](#)).

To assay inhibition of Bax, the fluorescence increase due to liposome permeabilization was measured (excitation at 355 nm and emission 520 nm) on a Tecan M1000 microplate reader. To ensure the background signal stabilized and to correct for compound fluorescence the initial fluorescence (F_0) was recorded for 15–30 min at 37°C in the presence of compounds and liposomes before adding proteins. Bax and tBid were added (in that order) at t_0 , and fluorescence changes (F) were measured for at least 2 h at 37°C. To estimate F_{100} , Triton X-100 was added to a final concentration of 0.2% (w/v), and fluorescence was measured for 10 min at 37°C. The change in hydrophobicity due to the addition of detergent results in a slight overestimation of F_{100} . The percentage release of ANTS/DPX was calculated as $[(F - F_0)/(F_{100} - F_0)] \times 100$. For compound screening, % inhibition was calculated by $[(\% \text{ Release}_{\text{Bax} + \text{tBid}} - \% \text{ Release}_{\text{Bax} + \text{tBid+ compound}})/\% \text{ Release}_{\text{Bax} + \text{tBid}}] \times 100$. Z-scores were calculated by $[(\% \text{ inhibition} - \% \text{ inhibition}_{\text{population mean}})/\text{Standard deviation}]$. Unless indicated otherwise, all assays used 20 nM tBid and 100 nM Bax.

Small Molecule Bax Inhibitor Screen

A collection of benzofuran-based flavonoid-inspired, and several tetrahydroquinoline alkaloid-inspired compounds were screened for inhibition of tBid/Bax-mediated dye release in a MOMP-mimicking liposome permeabilization assay. In the first round 86 compounds were individually added to liposomes and then purified Bax and tBid were added to induce permeabilization of liposomes. Small molecules that inhibited liposome permeabilization with a Z-score >2 were re-assayed manually. The top two compounds were used to select additional compounds for a second round of screening.

Compounds and Synthesis

Diversity-oriented synthesis of the compounds screened including MSN-125, MSN-50 and the synthesis of DAN004 are described in the [Methods S1](#). Nutlin-3a was obtained from Selleck.

Mitochondria Isolation and Permeabilization Assay

BMK Mitochondria

Bax^{-/-}/Bak^{-/-} or *Bax^{-/-}* baby mouse kidney (BMK) cells stably expressing a fusion protein comprised of the mitochondrial import peptide of Smac (amino acids 1–58) fused to the amino-terminus of the red fluorescence protein, mCherry were maintained in 3 µg/ml Blasticidin (Bioshop) in DMEM containing 10% FBS (Life Technologies). Heavy membranes containing mitochondria were isolated and assayed as described previously ([Shamas-Din et al., 2014](#)). Briefly, cells were lysed by nitrogen cavitation at 150 psi for 10 min on ice in buffer containing 20 mM HEPES (pH 7.2), 250 mM sucrose, 150 mM potassium chloride, 1 mM EDTA, 1 X protease inhibitor cocktail. Nuclei and cell debris were removed by centrifugation of the lysate at 2000g for 4 min at 4°C. Heavy membranes containing mitochondria were obtained by centrifuging the supernatant at 13000g for 10 min at 4°C and washing the pellet once in lysis buffer. Membrane fractions (0.2 mg/ml protein) were incubated with the compound, followed by the addition of 2 nM tBid and 20 nM Bax for the *Bax^{-/-}/Bak^{-/-}* mitochondria, or 0.5 nM tBid for the *Bax^{-/-}* mitochondria for 30 min at 37°C. Mitochondria were then pelleted by centrifugation at 13000 g for 10 min. The release of Smac-mCherry was assessed by fluorometric analysis of the supernatant and pellet fractions at excitation of 580 nm and emission of 610 nm in a Tecan M1000 microplate reader. The percentage release of Smac-mCherry was calculated as $[F_{\text{supernatant}} / (F_{\text{supernatant}} + F_{\text{pellet}})] \times 100$.

Mouse Liver Mitochondria

Mitochondria were isolated from livers of, *Bak^{-/-}* or wt mice and frozen as described ([Yamaguchi et al., 2007](#)). Briefly, mouse livers were lysed by dounce homogenization in AT buffer containing 300 mM Trehalose, 10 mM HEPES-KOH (pH 7.5), 10 mM potassium

chloride, 1 mM EGTA, 1 mM EDTA and 0.1% (w/v) BSA. Tissue components were removed by centrifugation at 600g for 10 min. To obtain heavy membranes containing mitochondria, the supernatant was centrifuged at 3500g for 15 min. The pellet was resuspended in AT buffer and centrifuged at 1500g for 5 min. The resulting supernatant was centrifuged at 5500g for 10 min (step performed twice). Mitochondrial fractions (50 mg/ml) were frozen at -80°C. When required, mitochondrial samples were thawed rapidly, washed in AT buffer containing 80 mM potassium chloride and resuspended in wash buffer supplemented with 5 mM succinate, 2 mM ATP, 10 µM phosphocreatine and 10 µg/ml creatine kinase.

To test inhibition of Bak by DAN004, mitochondria were isolated from wt mouse liver to remove endogenous Bax. After thawing, membrane fractions (1 mg/ml protein) were incubated with compound and 5 nM cBid and pelleted as described above. The supernatant and pellet fractions were analyzed by immunoblotting using a cytochrome c antibody affinity purified in our laboratory. Immunoblots were developed using chemiluminescence and intensities were recorded using a CCD camera (DNR). Image analysis was conducted using ImageJ to quantify the release of cytochrome c.

To measure mitochondrial permeabilization for constitutively active Bak protein synthesized in SP6 RNA polymerase/reticulocyte lysate-based transcription and translation coupled system, 40 µM MSN-50 was added to 2 µl Bak prior to the addition of mitochondria and cytochrome c release was assayed by ELISA (Zhang et al., 2016). As a control, inhibition was measured after addition of 2 µl Bcl-XL synthesized in vitro instead of MSN-50.

Long Term Survival after Replating

For experiments with MSN-125 and MSN-50 male HCT-116 (Wang and Youle, 2012) and BMK cells (Mathew et al., 2008) of unspecified sex were seeded at a cell density of 3000 cells/well in a 96 well plate (Sarstedt). For experiments with DAN004 BMK cells were seeded at 750 cells/well in 384 well plates. Cells were plated in in DMEM (Life Technologies) containing 10% FBS (Sigma) and after adhering, cells were treated with the indicated concentration of the inhibitors for 3-4 hours followed by addition of actinomycin D (ActD) (Sigma) or staurosporine (STS) for another 4 hours. The ActD/STS (+ compound) containing media was then replaced with drug-free media (containing inhibitor) and cells were grown for 4 days (to confluence for DMSO controls) and re-plated into 24 or 96 well plates (Sarstedt) for MSN and DAN004 inhibitors, respectively. Surviving cells were allowed to grow until the DMSO controls on the same plate just reached confluence and then the plate was stained with crystal violet (Sigma). Images of the plates were obtained using a flat-bed scanner. For 96 well plates, quantification of surviving cells was done by absorbance measurements at 600 nm as described previously (Brahmbhatt et al., 2016).

Immunofluorescence

HCT-116 cells were pre-treated with 10 µM MSN-125 for three hours, followed by the addition of actinomycin D (50 ng/ml final) for 24 hours. Cells were fixed using paraformaldehyde and analyzed by immunofluorescence by double staining with primary sheep anti-cytochrome c antibody (Capriologics) and mouse anti-Bax 6A7 monoclonal antibodies. Secondary donkey anti-sheep-Alexa Fluor 488 and goat anti-mouse-Alexa Fluor 555 (Invitrogen) antibodies were used for microscopy. The nuclei of HCT-116 cells were stained with DAPI according to the manufacturer's instructions (Sigma). Cells were imaged using a Zeiss LSM710 confocal microscope and associated software.

Primary Neuronal Cultures

All animal procedures were performed in accordance with the local standards for animal care and were approved by the animal care committee at Sunnybrook Research Institute. To establish primary neuron cultures of mixed sex, cerebral cortices from male and female mouse embryos (embryonic day E14.5-15) were dissected and cultured for up to 10 days to ensure maturation of neurons as described (Mergenthaler et al., 2012). Neurons from one embryo were considered as one independent "n". A maximum of 3 embryos of the same litter were used. Briefly, neurons were cultured in Neurobasal-A medium (Life Technologies) supplemented with B-27 (Life Technologies), 0.5 mM L-glutamine and 25 µM glutamate. The medium was partially replaced on day 6 in culture with Neurobasal-A supplemented with B-27 and L-glutamine. On day 9, neurons were treated with either 25 µM or 100 µM glutamate in BSS0 (116 mM NaCl, 5.4 mM KCl, 0.8 mM MgSO₄, 1 mM NaH₂PO₄, 26.2 mM NaHCO₃, 10 µM glycine, 1.8 mM CaCl₂, 10 mM HEPES pH 7.4) for 30 minutes (37°C, 5% CO₂) after washing the cultures with PBS. Medium was pooled and added to cultures after the incubation period with or without addition of 5 µM MSN-125. Cell death was analyzed 20-24 hours after glutamate treatment by measuring lactate dehydrogenase release as previously described (Mergenthaler et al., 2012). Briefly, lactate dehydrogenase concentration in medium was analyzed by measuring NADH to NAD⁺ turnover (absorbance at 340 nm) in a coupled spectrophotometric assay on a Tecan M1000 microplate reader at 37°C and normalized to total lactate dehydrogenase levels after volume correction. For each measurement, 200 µl LDH buffer (33 mM KH₂PO₄, 66 mM K₂HPO₄) containing 210 µM β-NADH (Sigma), pH 7.4 were added to 50 µl media supernatant in a 96 well plate. Immediately before starting the measurements, 25 µl LDH buffer containing 22.7 mM sodium pyruvate were added. Total lactate dehydrogenase release was measured after incubating neuronal cultures with 0.5% TritonX-100 for 30 minutes (37°C). All measurements were normalized to control reactions containing 500 units/l l-lactic dehydrogenase (Sigma). Statistical analysis was performed in Prism 5.0 (GraphPad) or SPSS 23 (IBM). ANOVA was performed after normality testing.

Bax:Bax Bax:Membrane FRET Assay

Bax:Bax or Bax:Membrane binding was assessed in a PTI Quantamaster fluorimeter using the FRET assay described previously (Lovell et al., 2008). For Bax:Bax FRET measurements, compounds dissolved in DMSO or as controls equivalent volumes of

DMSO were added after liposomes but prior to the proteins, thereby allowing correction for compound fluorescence. Liposomes were then incubated with DAC-134C-Bax and Initial fluorescence (F_0) was recorded (excitation, 380 nm and emission, 460 nm). Decreased DAC fluorescence (F) due to FRET was measured after the addition of NBD-126C-Bax and tBid.

For Bax:membrane FRET measurements, 10 μ M DAN004 was incubated with 20 nM of the donor-labeled protein, Alexa568-126C-Bax at 37°C for 10 minutes before adding 20 nM BIM and liposomes that were reconstituted in the presence of the acceptor fluorophore DiD (1,1'-Diocadecyl-3,3',3'-tetramethylindodicarbocyanine perchlorate; Life Technologies). DiD is incorporated into the reconstituted bilayer, and can be used as the acceptor for proteins binding membranes as previously described (Shamas-Din et al., 2013). FRET was measured by recording the initial fluorescence intensity (F_0 ; excitation, 580 nm and emission, 595 nm) of Alexa568-Bax incubated with DAN004. The fluorescence intensity of Alexa568-Bax decreased upon addition of the acceptor, DiD incorporated liposomes (F) due to FRET.

Disuccinimidyl Suberate (DSS) Crosslinking

Samples containing liposomes (125 μ M total lipids) were incubated with the compounds, 5 nM tBid and 100 nM Bax at 30°C for 2 hours in a low protein binding microtiter plate (Corning). DSS (Pierce) was added (2 mM final concentration) for 30min at room temperature followed by quenching with 20 mM Tris-Cl (pH 8) as described (Billen et al., 2008). Proteins were separated by SDS-PAGE and Bax was detected by immunoblotting with the monoclonal antibody 2D2 at a dilution of 1:10,000. Immunoblots were digitized by imaging with a CCD camera and the intensity of the dimer and larger oligomer bands was analyzed using ImageJ. To combine the data from multiple independent experiments the blots were normalized using the total intensity of dimer and larger oligomers in the “no compound” lane. Oneway ANOVA statistical test was performed in GraphPad Prism.

Disulfide Crosslinking

The single-cysteine Bax mutants were constructed and designated as described before (Zhang et al., 2016). The [35 S]Met-labeled Bax or Bak mutant proteins were synthesized in either a wheat germ-based in vitro translation (IVT) system or a transcription/translation (TNT) coupled SP6 RNA polymerase/reticulocyte lysate system (Promega) as described (Zhang et al., 2016). After adding 20 μ g/ml of cycloheximide to terminate translation, 15 or 7 μ l of the resultant Bax or Bak proteins from the IVT or TNT system, respectively, were mixed with mitochondria containing 0.5 mg/ml total protein. Mitochondria purified from liver of mice lack Bax as it is a cytosolic protein in liver. Mitochondria were treated with 18 mM N-ethylmaleimide (NEM) to block the sulphydryl groups of mitochondrial proteins, thereby preventing them from crosslinking with the cysteine(s) in Bax or Bak mutants via disulphides in the following oxidation reactions. In addition, 40 μ M MSN-50 or MSN-125, 1 mM DTT and for reactions containing Bax, 16 μ M of a peptide containing residues 53-86 of Bax including the BH3-region (BH3-peptide) that activates Bax (Tan et al., 2006), were added and the samples were incubated at 37°C for 1 h. The resulting mitochondria and bound Bax or Bak were pelleted by centrifugation at 4°C and 13,000 g for 5 min, and then resuspended in 100 μ l buffer A (110 mM KOAc, 1 mM Mg(OAc)₂ and 25 mM Hepes, pH 7.5). The resulting samples were treated with 1 mM NaAsO₄ to eliminate the residual DTT, and then divided into two aliquots. One aliquot was treated with redox catalyst copper (II) (1,10-phenanthroline)₃ (CuPhe; consisting of 0.3 mM CuSO₄ and 1 mM 1,10-phenanthroline) to induce disulfide crosslinking. After incubation on ice for 30 min, the oxidation reactions were quenched with 18 mM NEM, 100 mM ethylenediaminetetraacetic acid (EDTA) and 1 mM NaAsO₄. As the “0 min” control, the other aliquot was treated with NEM, EDTA and NaAsO₄ to block the disulfide crosslinking prior to the addition of CuPhe. The resulting samples were precipitated with Cl₃CCOOH, and then analyzed with non-reducing and as controls (not shown) reducing SDS-PAGE (15%), followed by phosphor-imaging to detect the radioactive Bax proteins and their disulphide-linked dimers. Intensities of both dimer and monomer bands in the phosphor-imaging data were measured and used to calculate the fraction of dimer. The fraction of dimer for each Bax or Bak sample in the absence or presence of a MSN compound was normalized to the mean fraction of dimer in the absence of the MSN compound from two to three independent experiments.

QUANTIFICATION AND STATISTICAL ANALYSIS

See individual sections above for details on the statistics used for analysis.

Supplemental Information

A Small-Molecule Inhibitor of Bax and Bak

Oligomerization Prevents Genotoxic Cell

Death and Promotes Neuroprotection

Xin Niu, Hetal Brahmbhatt, Philipp Mergenthaler, Zhi Zhang, Jing Sang, Michael Daude, Fabian G.R. Ehlert, Wibke E. Diederich, Eve Wong, Weijia Zhu, Justin Pogmore, Jyoti P. Nandy, Maragani Satyanarayana, Ravi K. Jimmidi, Prabhat Arya, Brian Leber, Jialing Lin, Carsten Culmsee, Jing Yi, and David W. Andrews

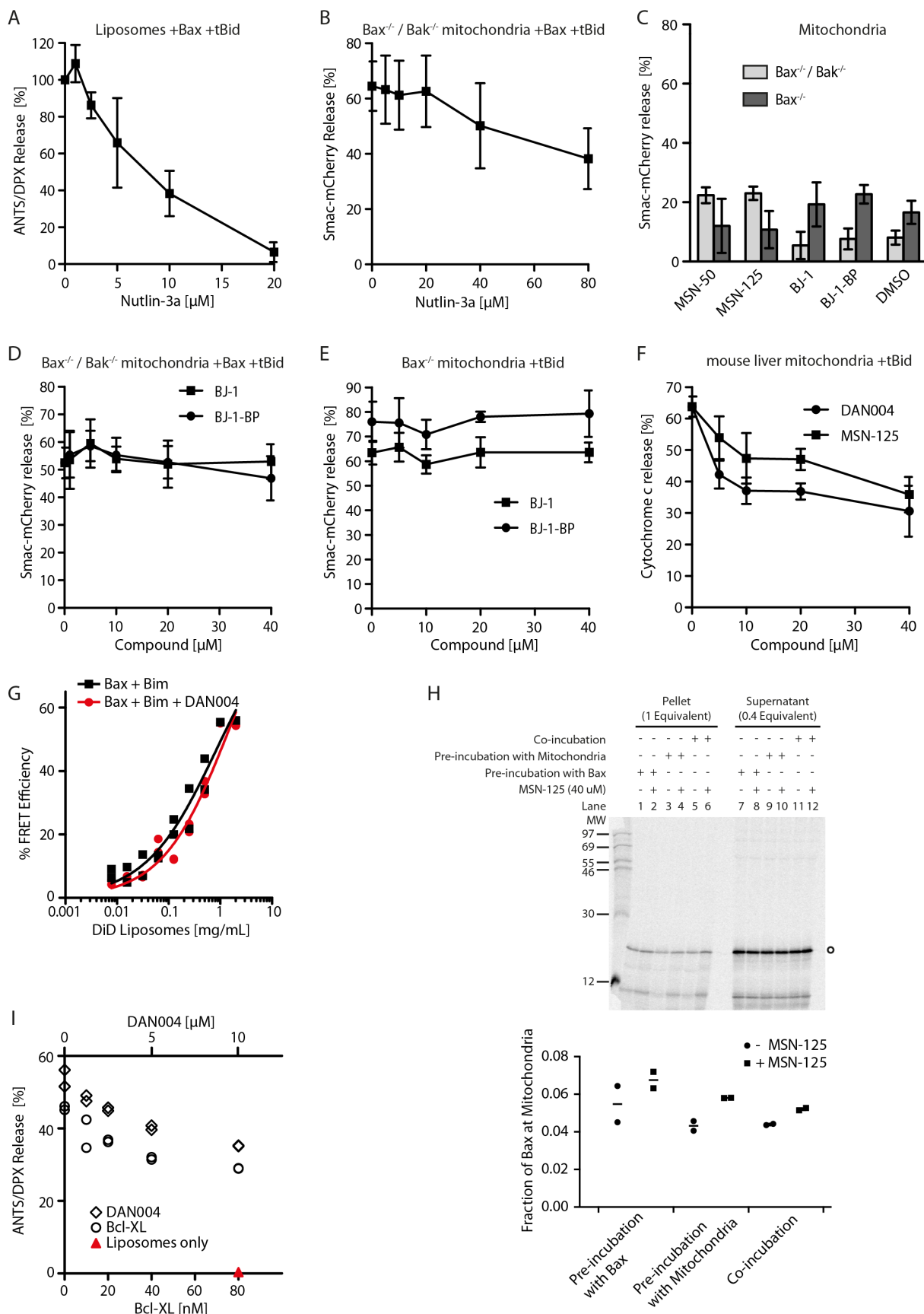


Figure S1. Effect of different compounds on membrane binding and permeabilization activities of Bax and Bak, Related to Figure 2

(A, B) Nutlin-3a inhibits Bax mediated permeabilization of liposomes and mitochondria.

(A) Inhibition of cBid and Bax mediated ANTS/DPX release from liposomes by the indicated concentrations of Nutlin-3a. Mean \pm SD, n=3. **Unless specified otherwise, in all supplementary figures n indicates the number of independent experiments.**

(B) Inhibition of cBid and Bax mediated release of Smac-mCherry from *Bax*^{-/-}/*Bak*^{-/-} mitochondria by the indicated concentrations of Nutlin-3a. Mean \pm SD, n=3.

(C) Controls illustrate that 40 μ M of the indicated compounds did not permeabilize *Bax*^{-/-}/*Bak*^{-/-} or *Bax*^{-/-} mitochondria. Mean \pm SD, n=3.

(D-F) DAN004 inhibits but BJ-1 and BJ-BP do not inhibit MOMP.

(D) BJ-1 and BJ-1-BP did not prevent tBid and Bax from releasing Smac-mCherry from mitochondria isolated from *Bax*^{-/-}/*Bak*^{-/-} BMK cells. Mean \pm SD, n=3.

(E) BJ-1 and BJ-1-BP did not prevent exogenous tBid and endogenous Bak from releasing Smac-mCherry from *Bax*^{-/-} mitochondria isolated from BMK cells. Mean \pm SD, n=3.

(F) DAN004 and MSN-125 inhibit exogenous tBid and endogenous Bak mediated release of cytochrome c from mitochondria that do not contain Bax, isolated from mouse liver. Permeabilization was measured by % of cytochrome c released from the mitochondria determined by immunoblotting pelleted mitochondria and supernatants. Mean \pm SD, n = 3.

(G) Preincubation of Alexa568-labeled BAX-126C (20 nM) and DAN004 (10 μ M) at 37°C for 10 minutes before adding reconstituted DiD liposomes does not inhibit Bax binding to liposomes as measured by FRET.

(H) MSN-125 does not inhibit Bax binding to mitochondria isolated from Bak^{-/-} mouse liver. Bax or mitochondria were pre-incubated with 40 μ M MSN-125 or DMSO (for - MSN-125 sample) for 15 min at 22 °C as specified and then 0.2 mg/ml mitochondria or 2.5 μ l radioactive Bax synthesized by in vitro transcription/translation and 20 nM cBid were added and incubated for 60 min at 37 °C. For co-incubation all components were mixed together and incubated accordingly. Both mitochondria pellets and supernatants were collected after centrifugation and subjected to SDS-PAGE and phosphorimaging to detect radioactive Bax. The fractions of Bax bound to mitochondria calculated from band intensities in the pellet and supernatant for two independent experiments are presented below the gel image as circles and squares with dashes for the means.

(I) DAN004 inhibits membrane permeabilization mediated by heat activated Bax. After incubation of 120 nM of Bax with the indicated concentrations of DAN004 or as a control, Bcl-XL, liposomes were added. The temperature was raised to 55° C for 30 minutes and permeabilization was measured as %ANTS/DPX release from liposomes. Individual data points are means of duplicate samples for two independent experiments.

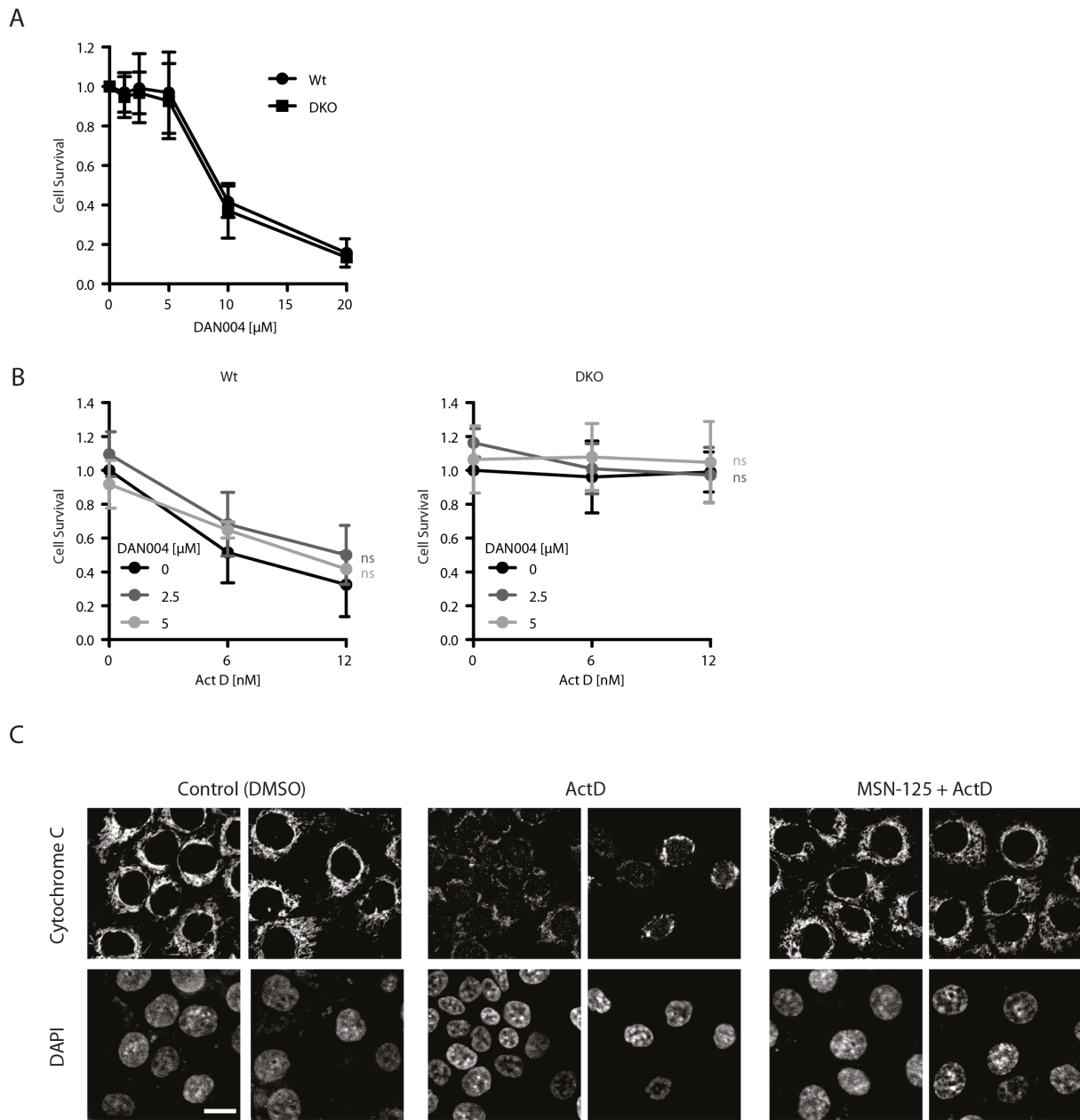


Figure S2. Unlike MSN-125, DAN004 does not protect cells from apoptosis induced by ActD, Related to Figure 3

(A-B) DAN004 kills Wt and DKO cells and does not confer protection against ActD.

(A) Cell viability of HCT-116 Wt and *Bax*^{-/-}/*Bak*^{-/-} DKO cells exposed to DAN004 for 8 hours. Cells were replated after 4 days and grown till the “DMSO” treated cells were confluent. Surviving cells were stained with crystal violet. Results are normalized to DMSO treated controls. Mean ± SD, n=4 independent experiments.

(B) HCT-116 Wt and DKO cells treated with DAN004 for 4 hours followed by treatment with both DAN004 and the indicated doses of ActD for 4 hours. After 4 days cells were replated and cell survival was assessed as described above. Statistical analysis was conducted using two-way ANOVA with the Bonferroni post-test comparing DAN004-treated cells versus untreated cells. ns = non-significant for P values >0.05; Mean ± SD, n = 3 independent experiments.

(C) MSN-125 prevents ActD mediated cytochrome c release from ActD treated HCT-116 cells. HCT-116 cells were treated with 10 μM MSN-125 for 3 hours before ActD treatment for 24 hours. Nuclear shrinkage observed for ActD treated cells is also reduced by MSN-125. Cells were fixed and immunofluorescence was performed with primary antibodies against cytochrome c. Nuclei were visualized using DAPI. The scale bar indicates 10 μm.

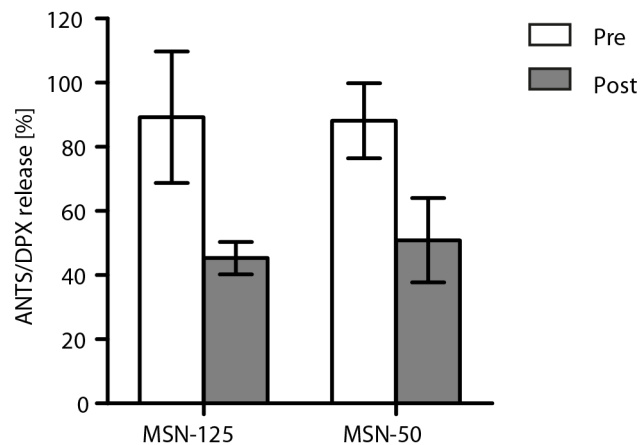


Figure S3. MSN-50 and MSN-125 do not inhibit liposome permeabilization by partitioning into the membrane, Related to Figure 4

Liposomes pre-incubated with 10 μ M MSN-125 or MSN-50 and passed over a gel filtration column to remove unpartitioned compound ("Pre") released ANTS/DPX in response to tBid and Bax. In control reactions in which MSN-125 or MSN-50 was added after liposomes were passed over the column ("Post") ANTS/DPX release was inhibited.

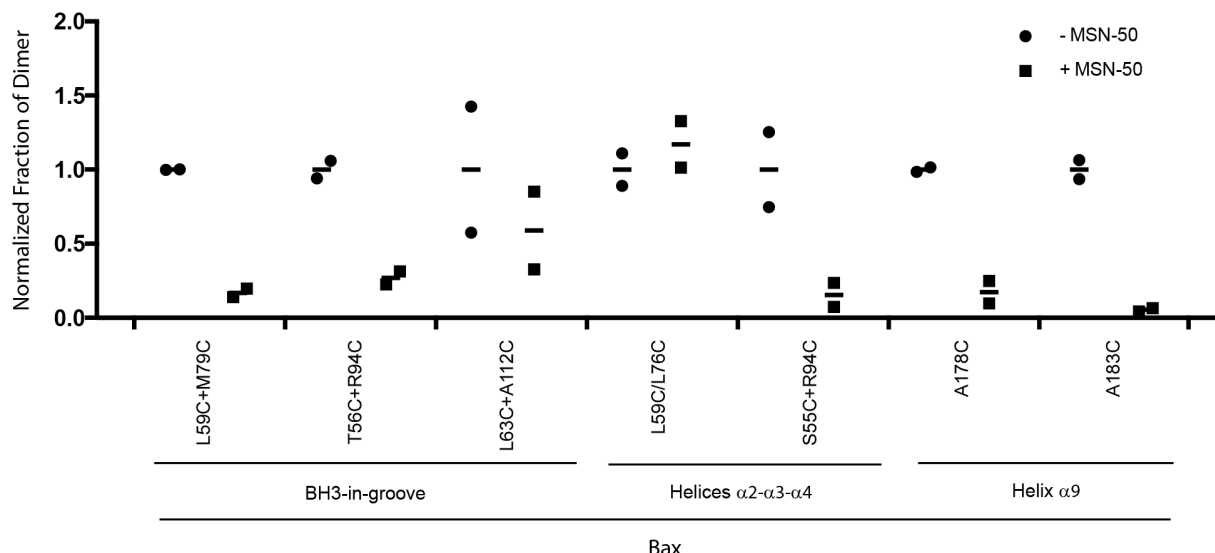
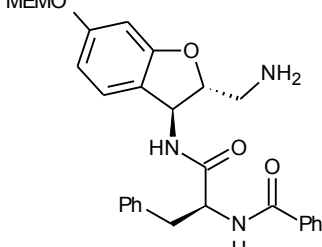
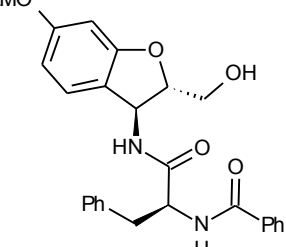
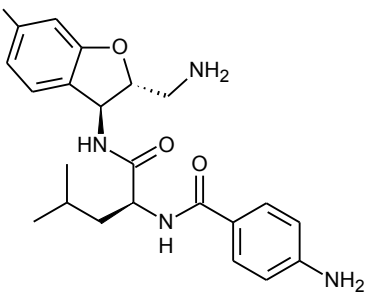
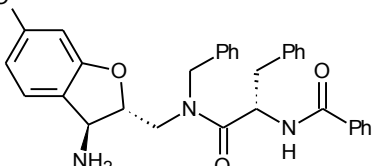
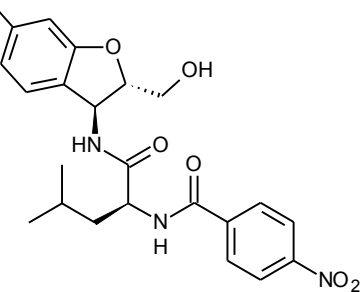
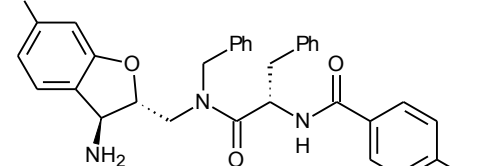


Figure S4. MSN-50 inhibits some, but not all, interactions in Bax dimers, Related to Figure 5

While disulphide linkage of L59C/L76C was resistant to MSN-50, linkages of the other sites were inhibited by MSN-50, similar to the data for MSN-125 shown in Figure 5B. The only exception is the linkage of L63C with A112C that is partially blocked by MSN-50 but fully blocked by MSN-125. Intensities of both dimer and monomer bands were obtained from phosphorimager data for disulfide crosslinking of single-cysteine Bax mutant pairs (e.g., L59C+M79C) or the double-cysteine Bax mutant (L59C/L76C) incubated with mitochondria lacking endogenous Bax and Bak, isolated from Bak^{-/-} mouse liver, in the absence or presence of MSN-50. This data was used to calculate the mean fraction of dimer in the absence of MSN-50 and the corresponding normalized fraction of dimer after treatment with inhibitor. Circles and squares represent individual data points with the mean indicated by a dash. Data from n = 2 independent experiments is shown.

Supplemental Table S1. Related to Figure 2

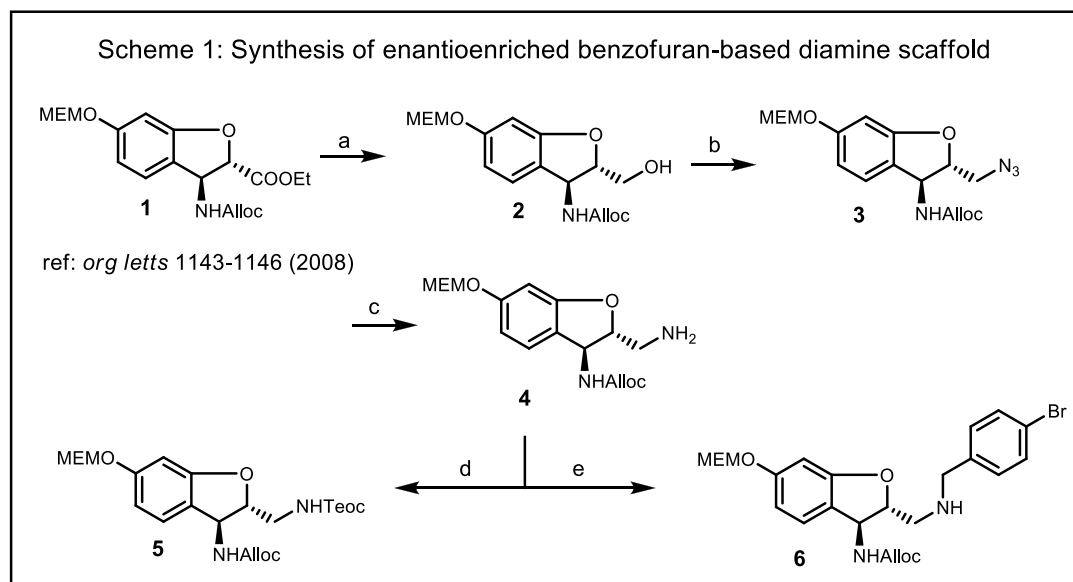
Liposomes permeabilization by 10 µM of the compounds cBid and Bax.

Compound ID:	Structure	ANTS/ DPX Release [%]
ILS-JRK-3-37		68
ILS-JRK-3-41		91
ILS-JRK-3-45		94
ILS-JRK-3-31		45
ILS-JRK-3-39		104
ILS-JRK-3-29		94

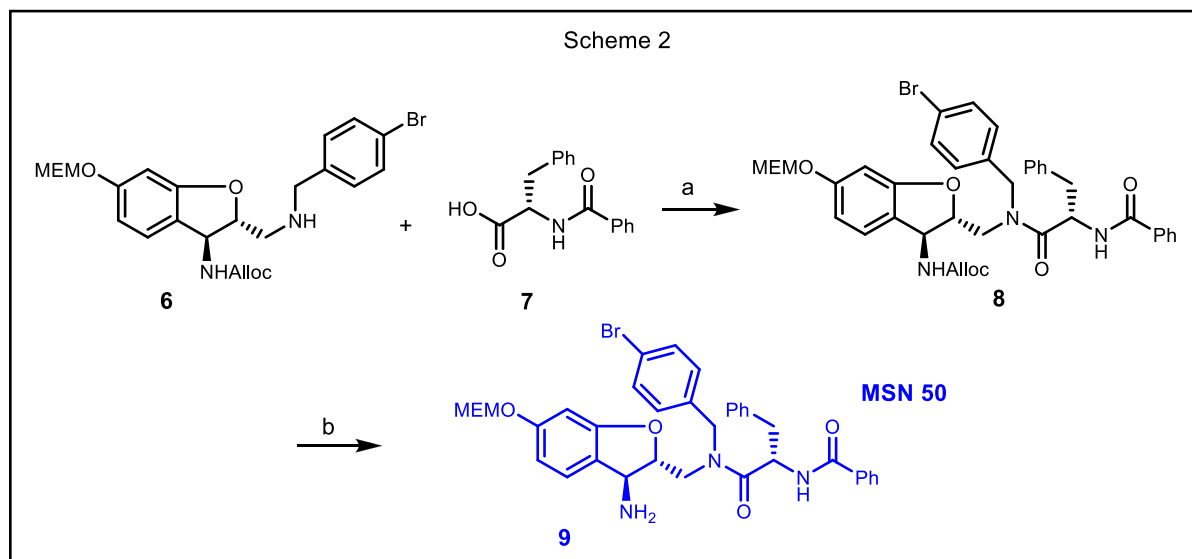
ILS-JRK-3-34	<p>MEMO</p>	95
ILS-JRK-3-32	<p>MEMO</p>	145
ILS-JRK-C95-124 (1)	<p>MEMO</p>	93
ILS-JRK-C95-140	<p>MEMO</p>	93
ILS-JRK-C95-182	<p>MEMO</p>	76

METHODS S1. Synthesis of MSN-50, MSN-125 and DAN004

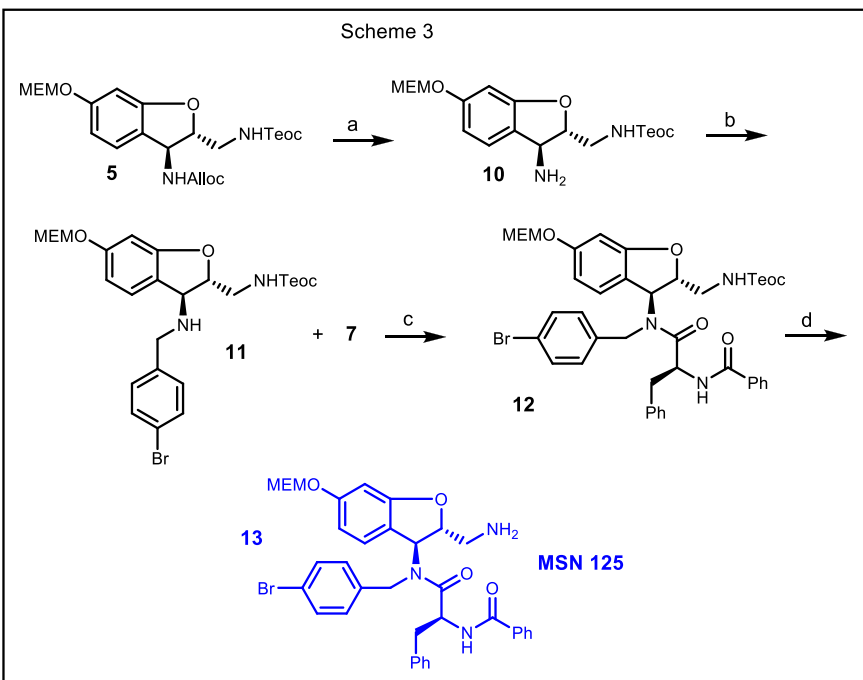
1) Experimental Section for the Synthesis of Small Molecules MSN-50 and MSN-125



Reagents and conditions: a) LiBH₄, THF, 0 °C to rt, 2 h; b) DPPA, TPP, DEAD, THF, 0 °C, 2h; c) TPP, H₂O, THF, rt, 12 h; d) triphosgene, trimethylsilyl ethanol, py, CH₂Cl₂, 0 °C, 4h; e) *p*-bromobenzaldehyde, NaCNBH₃, TMOF, AcOH, MeOH, rt, 4 h.

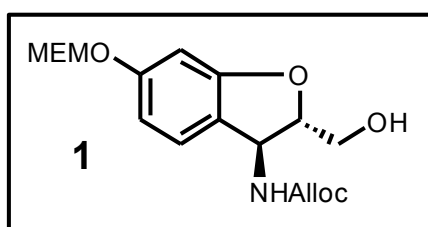


Reagents and conditions: a) PyBop, DIPEA, CH₂Cl₂, rt, 12 h; b) Pd(PPh₃)₄, morpholine, CH₂Cl₂, 0 °C to rt, 2 h.

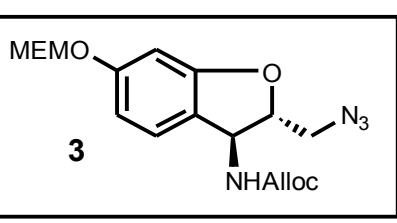


Reagents and conditions: a) $\text{Pd}(\text{PPh}_3)_4$, morpholine, CH_2Cl_2 , 0°C to rt, 2h; b) *p*-bromobenzaldehyde, NaCNBH_3 , TMOF, AcOH , MeOH , rt, 4 h; c) PyBop, DIPEA, CH_2Cl_2 , rt, 12 h; d) TBAF , THF , 0°C to rt, 2 h.

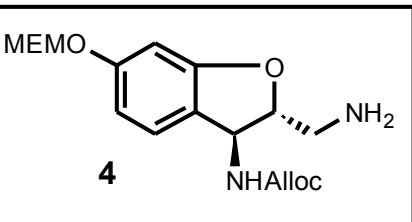
Experimental Section



To a stirred solution of compound **1** 0.5 g, 1.26 mmol) in dry THF (10 mL) was added a solution of 2M LiBH_4 in THF of (0.62 mL, 1.26 mmol) at 0°C under inert atmosphere. The reaction was allowed to warm to room temperature and stirred for 3 hours. The reaction mixture was quenched by addition of a saturated *aq.* NH_4Cl , extracted with ethyl acetate, washed with brine, dried over anhydrous MgSO_4 and concentrated *in vacuo*. Purification by flash chromatography (40% ethyl acetate in hexane) afforded compound **2** (0.38 g, 80 %) as a white solid. ^1H NMR (CDCl_3 , 400 MHz): 3.21 (s, 3H), 3.39 (m, 2H), 3.81-3.88 (m, 4H), 4.59-4.61 (m, 3H), 5.14-5.35 (m, 6H), 5.90-5.94 (m, 1H), 6.58 (s, 1H), 6.63 (d, $J = 2.0$ Hz, 1H), 7.16 (d, $J = 2.0$ Hz, 1H); ^{13}C NMR (CDCl_3 , 100 MHz): 56.0, 59.4, 63.9, 66.5, 68.1, 71.9, 91.8, 93.9, 98.4, 99.4, 109.9, 118.6, 118.7, 125.8, 132.7, 156.5, 160.0, 161.2; MS: (ES+) $m/z = 354$ ($m+1$), HPLC purity (>97%).

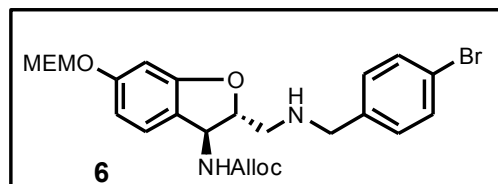


To a solution of alcohol **2** (0.047 g, 0.097 mmol) in 3.88 mL of THF was added triphenylphosphine (0.026 g, 0.099 mmol), DEAD (0.019 mL, 0.099 mmol), and diphenylphosphoryl azide (0.021 mL, 0.099 mmol) at 0°C and stirred for 3 hours. The reaction was quenched with saturated NaHCO_3 and extracted with ethyl acetate (3 x 10 mL). The combined organics were dried over anhydrous Mg_2SO_4 , concentrated *in vacuo* and purified by silica gel column chromatography to afford azide **3** (0.042 g, 85%) as brownish liquid. ^1H NMR (CDCl_3 , 400 MHz): 3.39 (s, 3H), 3.50-3.60 (m, 3H), 3.70-3.74 (m, 1H), 3.81-3.84 (m, 2H), 4.61 (d, $J = 5.52$ Hz, 2H), 4.65-4.69 (m, 1H), 5.04-5.07 (m, 1H), 5.12-5.14 (m, 1H), 5.25-5.27 (m, 3H), 5.28-5.35 (d, $J = 17.5$ Hz, 1H), 5.87-5.98 (m, 1H) 6.62 (d, $J = 2.0$ Hz, 1H), 6.65-6.68 (m, 1H), 7.17-7.19 (m, 1H); ^{13}C NMR (CDCl_3 , 100 MHz): 53.8, 56.1, 59.4, 66.3, 68.2, 71.9, 90.2, 94.0, 99.5, 110.1, 118.4, 125.7, 132.8, 156.0, 160.2, 161.1; MS: (ES+) $m/z = 379$ ($m+1$), HPLC purity (>97%).



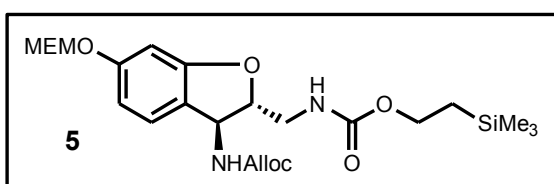
To a stirred solution of azide compound **3** (0.225 g, 0.595 mmol) in THF (3 mL) was added TPP (0.166 g, 0.636 mmol) and water (100 μL). The reaction mixture was left for stirring for 12 h at room temperature. After the completion of the reaction THF was

removed under vacuuo and purified by flash column using DCM, MeOH solvent system to afford pure amine **4** as colorless liquid in 80 % yield. ¹H NMR (CDCl₃, 400 MHz): 2.96-3.03 (m, 1H), 3.09-3.14 (m, 1H), 3.40 (s, 3H), 3.56-3.59 (m, 2H), 3.81-3.84 (m, 2H), 4.48-4.53(m, 1H), 4.62 (d, *J* = 5.0 Hz, 2H), 5.05-5.12 (m, 1H), 5.25-5.28 (m, 3H), 5.31-5.38 (d, *J* = 16.5 Hz, 1H), 5.87-5.99 (m, 1H), 6.57 (d, *J* = 2.0 Hz, 1H), 6.64 (dd, *J* = 2.5 Hz, 1H), 7.18 (d, *J* = 8.0 Hz, 1H); ¹³C NMR (CDCl₃, 100 MHz): 45.4, 56.1, 59.4, 66.2, 68.1, 71.9, 93.2, 94.0, 99.3, 109.6, 118.4, 119.3, 125.9, 132.9, 156.0, 160.0, 161.3. MS: (ES+) m/z = 353 (m+1), HPLC purity (>97%).



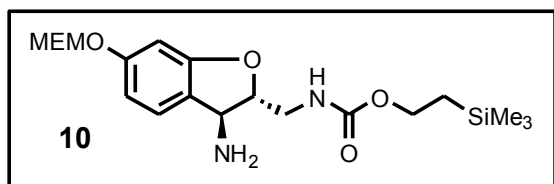
The pure amine **4** (0.318 g, 0.9 mmol) and *p*-bromobenzaldehyde (0.183 g, 0.993 mmol) dissolved in triethyl orthoformate (4.0 mL), and a solution of NaCNBH₄ (85 mg, 1.355 mmol) in TMOF/MeOH/AcOH (3 mL/720 μ L/80 μ L) was added to the above mixture at room temperature. The reaction mixture was stirred for 4 h. The reaction was quenched with saturated NH₄Cl solution and washed with water and brine. The organic layer was dried over sodium sulfate, filtered, and concentrated under reduced pressure. The crude product was purified by column chromatography on silica gel (1:1 ethyl acetate/hexanes) to give the product **6** (0.36 g, 77%).

¹H NMR (CDCl₃, 400 MHz): 2.90-2.95 (m, 1H), 3.0-3.04 (m, 1H), 3.39 (s, 3H), 3.56-3.58 (m, 2H), 3.81-3.83 (m, 4H), 4.60-4.65 (m, 3H) 5.03 (d, *J* = 7.5 Hz, 1H), 5.14-5.17 (m, 1H), 5.23-5.26 (m, 3H), 5.31-5.35 (m, 1H) 5.89-5.99 (m, 1H), 6.56 (d, *J* = 2.0 Hz, 1H), 6.61 (dd, *J* = 2.0 Hz, 1H), 7.16 (d, *J* = 8.5 Hz, 1H), 7.21 (d, *J* = 8.5 Hz, 1H) 7.44 (d, *J* = 8.5 Hz, 2H); ¹³C NMR (CDCl₃, 100 MHz): 52.1, 53.5, 56.6, 59.4, 66.2, 68.1, 71.9, 91.0, 94.0, 99.3, 109.7, 118.4, 119.3, 121.1, 125.9, 130.2, 131.8, 132.9, 139.5, 156.0, 160.0, 161.2; MS: (ES+) m/z = 521 (M+1), 523 (M+3) HPLC purity (>97%).



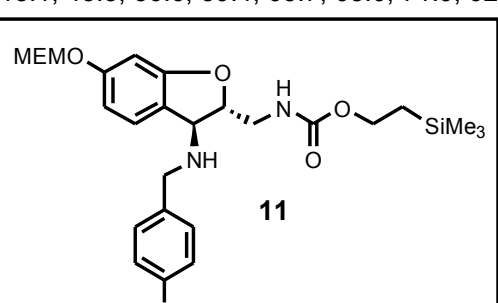
Triphosgene (33 mg, 0.112 mmol) was added to the round bottom flask and cooled to 0 °C. This was then followed by a slow addition of 3 mL of anhydrous CH₂Cl₂, and 2-(trimethylsilyl) ethanol (49 μ L, 0.34 mmol) was added in one portion to the reaction mixture. Then pyridine (27.6 μ L, 0.34 mmol) was added drop wise to the reaction mixture and

stirred for 2 h at 0 °C. Then a solution of free amine **4** (60 mg, 0.17 mmol) and pyridine (42 μ L, 0.51 mmol) in 3 mL of anhydrous CH₂Cl₂ was added via cannula over a period of 5 min. The mixture was stirred continuously for 2 h at 0 °C. When the TLC showed no starting material, the reaction mixture was quenched via the addition of a saturated solution of NaHCO₃, and the aqueous layer was extracted with CH₂Cl₂ (3 x 10 mL). The organic layer was dried over MgSO₄, filtered, and concentrated under vacuum, and the crude product was chromatographed on silica gel with (hexane/ ethyl acetate 7/3) to give **5** (77 mg, 91%) as a white solid. ¹H NMR (CDCl₃, 400 MHz): 1.0 (t, *J* = 8.5Hz, 2H), 3.4 (s, 3H), 3.5-3.59 (m, 4H) 3.81-3.84 (m, 2H), 4.18 (t, *J* = 8.5Hz, 2H), 4.57-4.63 (m, 1H) 5.03-5.09 (m, 1H), 5.25-5.27 (m, 3H), 5.31-5.35 (d, *J* = 17.0Hz, 1H), 6.57 (d, *J* = 2.0 Hz, 1H), 6.65 (dd, *J* = 2.0 Hz, 1H), 7.18 (d, *J* = 8.0 Hz, 1H); MS: (ES+) m/z = 497 (M+1), 498 (M+2) HPLC purity (>95%).



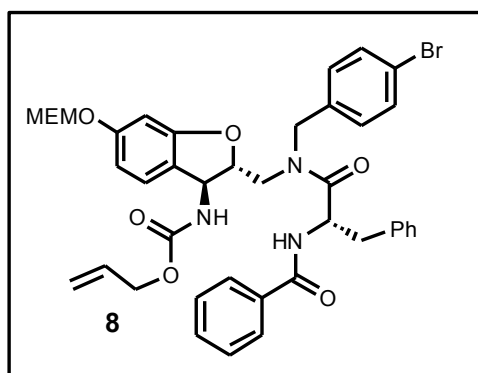
To a solution of **5** (77 mg, 0.155 mmol) in dry CH₂Cl₂ (5 mL) under organ atmosphere at 0 °C, was added morpholine (27.6 μ L, 0.317 mmol) and tetrakis(triphenylphosphine) palladium (0) catalyst (17.9 mg, 0.0158 mmol). The round-bottom flask containing the mixture was covered with aluminum foil and stirred for 1 h. TLC showed the completion

of the reaction. The solvent was evaporated to dryness and the crude mixture subjected to flash column chromatography to give pure benzylic amine **10** (60 mg, 95% yield). ¹H NMR (CDCl₃, 400 MHz): 0.05 (s, 9H), 0.99 (t, *J* = 8.53 Hz, 2H), 3.40-3.48 (m, 4H), 3.57-3.66 (m, 2H), 3.82-3.84 (m, 2H), 4.17(t, *J* = 8.51Hz, 2H) 4.29(d, *J* = 5.52 Hz, 1H), 4.37-4.41(m, 1H), 5.0 (bs, 1H), 5.25(s, 2H0, 6.54-6.66 (m, 1H), 6.64 (dd, *J* = 2.0, 2.5Hz, 1H), 7.18 (d, *J* = 8.53 Hz, 1H); ¹³C NMR (CDCl₃, 100 MHz): -1.0, 0.4, 18.1, 43.5, 56.6, 59.4, 63.7, 68.0, 71.9, 92.0, 94.0, 99.3, 109.6, 124.5, 125.2, 157.3, 159.3, 160.3; MS: (ES+) m/z = 413 (M+1), 395 (M-NH₃) HPLC purity (>96%).

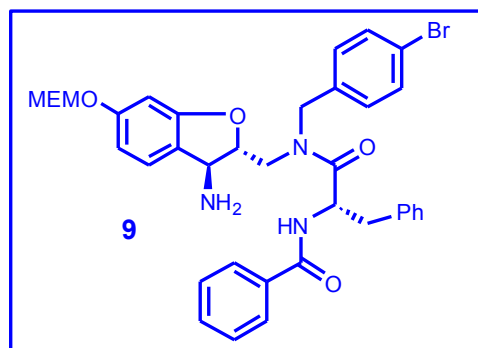


This compound is prepared following the similar procedure described for the compound **6** using the benzylic amine **10** (63 mg, 0.152 mmol), *p*-

bromobenzaldehyde (31 mg, 0.168 mmol) and NaCNBH₃/AcOH/MeOH (15 mg, 0.228 mmol/12 μ L/120 μ L) in TMOF to afford compound **11** (79 mg, 90% yield). ¹H NMR (CDCl₃, 400 MHz): 0.05 (s, 9H), 1.00(t, J = 8.03 Hz) 3.25-3.32 (m, 1H), 3.40 (s, 3H), 3.53-3.59 (m, 3H), 3.82-3.85 (m, 4H), 4.15-4.20 (m, 3H), 4.63-4.66 (m, 1H), 4.97 (m, 1H), 5.25(s, 2H), 4.63-4.66 (m, 1H), 4.97 (m, 1H), 5.25 (s, 2H), 6.57 (d1 J = 2.0, 1H), 6.62 (dd, J = 2.0, 2.5, 1H), 7.19(d, J = 8.03, H_z, 1H), 7.25-7.28 (m, 2H), 7.45-7.48 (m, 2H); ¹³C NMR (CDCl₃, 100 MHz): -1.0, 0.4, 18.1, 44.4, 50.2, 59.4, 62.0, 63.7, 68.1, 71.9, 88.7, 94.0, 99.4, 109.5, 121.3, 126.0, 130.2, 131.9, 159.5, 160.6; MS: (ES+) m/z = 581 (M+1), 583 (M+3) HPLC purity (>97%).

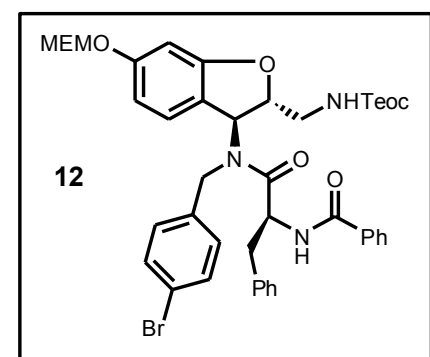


To a stirred solution of amine **6** (46 mg, 0.088 mmol) and amino acid **7** (28 mg, 0.106 mmol) in dry dichloromethane under organ atmosphere were added PyBrop (49 mg, 0.106 mmol) and DIPEA (31 μ L, 0.176 mmol) at room temperature. The reaction mixture was allowed to stir for overnight. After completion of the reaction as indicated by the TLC and LC-MS, organic layer evaporated and the crude mixture was dissolved in ethyl acetate (3x20 mL) and combined organic layers were concentrated and the crude mixture was purified by column chromatography using hexane and ethyl acetate (7:3) solvent system to give pure compound **8** (48 mg, 58% yield). ¹H NMR (CDCl₃, 400 MHz, 58 °C): 3.11-3.28 (m, 2H), 3.38-3.40 (m, 3H), 3.53-3.60 (m, 2H), 3.78-3.85 (m, 3H), 4.26-5.00 (m, 6H), 5.16-5.39 (m, 6H), 5.50 (bs, 1H), 5.83-6.00 (m, 1H), 6.49-6.76 (m, 3H), 6.83-7.00 (m, 2H), 7.11-7.28 (m, 4H), 7.35-7.54 (m, 6H), 7.71-7.82 (m, 2H); MS: (ES+) m/z = 772 (M+1), 774 (M+3) HPLC purity (>95%).

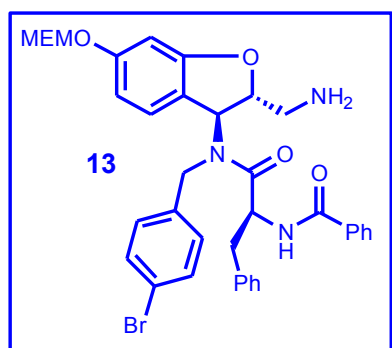


To a solution of **8** (48mg, 0.062 mmol) in dry CH₂Cl₂ (5 mL) under organ atmosphere at 0 °C, was added morpholine (10 μ L, 0.124 mmol) and tetrakis(triphenylphosphine) palladium (0) catalyst (7 mg, 0.0062 mmol). The round-bottom flask containing the mixture was covered with aluminum foil and stirred for 1 h. TLC showed the completion of the reaction. The reaction was quenched with saturated NH₄Cl solution and washed with water and brine. The organic layer was dried over anhy. MgSO₄, filtered, and concentrated under reduced pressure to give crude compound which upon flash column chromatography using ethyl acetate (100%) to afford amine **9** (40 mg, 95 % yield).

¹H NMR (CDCl₃, 400 MHz, 58 °C): 3.02-3.31 (m, 2H), 3.37 (m, 3H), 3.47-3.48 (m, 0.5H), 3.54-3.61 (m, 2.5H), 3.73-3.86 (m, 2.5H), 3.94-3.99 (m, 0.5H), 4.05-4.10 (m, 1H), 4.14-4.24 (m, 1H), 4.36-4.49 (m, 1H), 4.51-4.63 (m, 1H), 4.70-4.81 (m, 0.5H), 5.02-5.06 (m, 0.5H), 5.19-5.31 (m, 2.5H), 5.36-5.59 (m, 1H), 6.49-6.55 (m, 1H), 6.61-6.65 (m, 1H), 6.79-7.02 (m, 3H), 7.09-7.16 (m, 2H), 7.20-7.34 (m, 3H), 7.39-7.54 (m, 5H), 7.73-7.80 (m, 2H); MS: (ES+) m/z = 671 (M-NH₃+1), 673 (M-NH₃+3) HPLC purity (>97%).



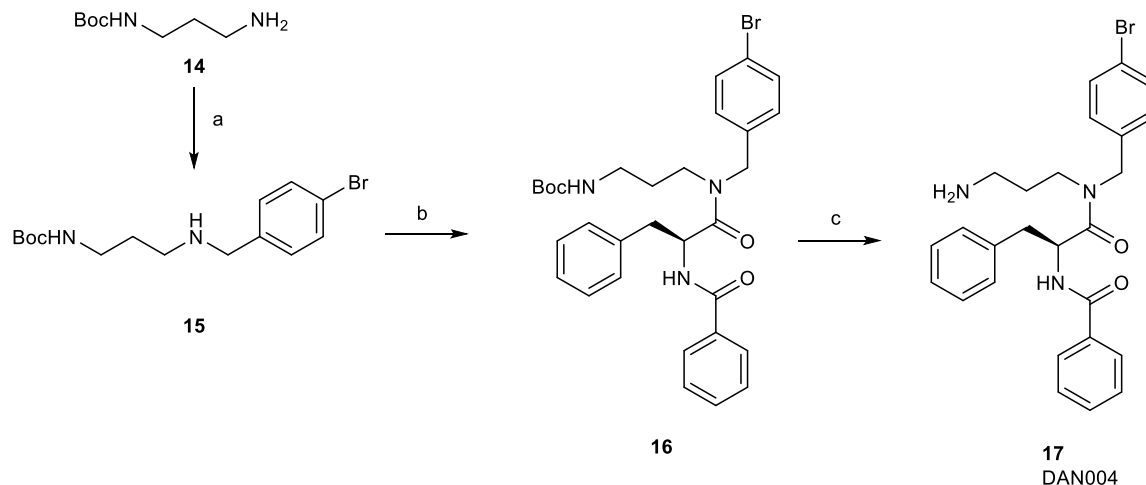
Compound **12** was prepared following the similar procedure described for the compound **8**, by using amine **11** (60 mg, 0.103 mmol), amino acid **7** (33 mg, 0.123 mmol), PyBrop (58 mg, 0.123 mmol) and DIPEA (36 L, 0.206 mmol) to afford the compound **12** (50 mg) 58 % yield. ¹H NMR (DMSO, 400 MHz, 120 °C): 0.01 (s, 9H), 0.89 (m, 2H), 3.05-3.17 (m, 2H), 3.22-3.34 (m, 5H), 3.48-3.50 (m, 2H), 3.71-3.74 (m, 2H), 4.02-4.06 (m, 2H), 4.20-4.36 (m, 3H), 4.52-4.65 (m, 2H), 5.16 (s, 2H), 5.72 (bs, 1H), 6.37-6.46 (m, 2H), 6.65-6.73 (bs, 1H), 6.89-7.00 (m, 3H), 7.17-7.35 (m, 6H), 7.41-7.53 (m, 4H), 7.78-7.85 (m, 2H), 8.48 (bs, 1H); MS: (ES+) m/z = 832 (M+1), 834 (M+3) HPLC purity (>97%).



To a stirred solution of compound **12** (40 mg, 0.047 mmol) in dry THF under organ atmosphere was added TBAF (0.1 mL, 0.095 mmol) solution in THF at 0° C. The reaction mixture was allowed to warm to rt and stirred for overnight. After completion of the reaction as indicated by TLC and LC-MS, the solvent was evaporated under vacuum to give crude product which was subjected to flash chromatography using dichloromethane and methanol (9.8:0.2) solvent system on triethylamine neutralized silica gel to give pure amine **13** (30 mg, 93 % yield). ¹H NMR (CDCl_3 , 400 MHz): 2.47-2.67 (m, 0.5 H), 2.83-3.03 (m, 1.5 H), 3.11-3.21 (m, 2H), 3.38-3.41 (m, 3H), 3.56-3.61 (m, 2H), 3.78-3.84 (m, 2H), 3.95-3.98 (m, 0.5), 4.14-4.27 (m, 2H), 4.36-4.47 (m, 0.5H), 5.19-5.28 (m, 2.5H), 5.69-5.83 (m, 1.5H), 6.46-6.54 (m, 2H), 6.69-7.02 (m, 4H), 7.14-7.16 (m, 1H), 7.25-7.35 (m, 4H), 7.45-7.57 (m, 4H), 7.77-7.81 (m, 2H); MS: (ES+) m/z = 688 (M+1), 690 (M+3) HPLC purity (>97%).

2) Experimental Section for the Synthesis of Small Molecule DAN004 (17)

Reductive amination of *tert*-butyl (3-aminopropyl)carbamate **14** with 4-bromobenzaldehyde gave rise to **15** the secondary amino functionality of which subsequently was coupled to *N*-benzoyl-*L*-phenylalanine yielding **16**. Final deprotection rendered **17** (DAN004) in good overall yield.



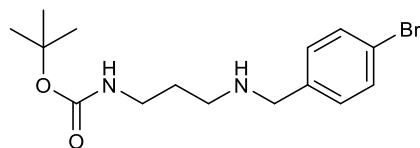
Reagents and conditions: a) 4-bromobenzaldehyde, NaBH₄, MeOH, 0°C → RT, 16 h 77%; b) *N*-benzoyl-*L*-phenylalanine, HBTU, *N*-methylmorpholine, DMF, RT, 14h, 61%; c) TFA, DCM, RT, 72h, 92%.

General synthesis

Commercially available reagents and solvents were used without further purification, except for cyclohexane which was distilled prior to use. Thin layer chromatography (TLC) was performed on precoated TLC-plates (silica gel 60 F254, Merck). Flash column chromatography was performed on prepacked flash chromatography columns (PF 30-SIHPJP/ 12G) purchased from Interchim using a Büchi separation system.

Melting points were determined using the melting point meter MPM-H2 (Schorpp Gerätetechnik, Germany) and are uncorrected. ¹H-NMR and ¹³C-NMR spectra were recorded either on a JEOL ECX-400 or a JEOL ECA-500 spectrometer. Chemical shifts (δ) are given in ppm with the residual solvent signal used as reference [¹H: DMSO-d₆ (30°C): quint, δ =2.49ppm; CDCl₃ (20°C): s, δ =7.26ppm; ¹³C: DMSOd₆ (30°C): quint, δ =39.50ppm, CDCl₃ (20°C): t, δ =77.16ppm]. Coupling constants (J) are reported in hertz (Hz). Peak patterns are abbreviated as follows: s (singlet), d (doublet), dd (double doublet), dt (doublet of triplet), t (triplet), m (multiplet), sm (symmetric multiplet), br (broad), ps (pseudo). Mass spectra were either recorded on a triple quadrupole spectrometer type EP 10+ (MS Vision), a triple quadrupole spectrometer type Q-Trap 2000 (Applied Biosystems), or on a double-focusing sector field spectrometer type AutoSpec (Micromass). Elemental combustion analyses were performed on a vario MICRO cube (Elementar Analysensysteme GmbH, Hanau, Germany).

tert-butyl (3-((4-bromobenzyl)amino)propyl)carbamate (**15**)

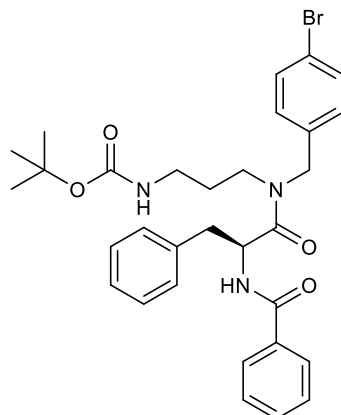


A solution of *tert*-butyl (3-aminopropyl)carbamate (**14**, 0.435 g, 2.50 mmol) and 4-bromobenzaldehyde (0.509 g, 2.75 mmol, 1.1 equiv.) in MeOH (10 mL) was stirred for 3h at RT under an argon atmosphere. The reaction mixture was subsequently cooled to 0 °C and sodium borohydride (0.378 g, 10.0 mmol, 4 equiv.) was added slowly, followed by further stirring of the mixture for additional 16h at RT. After concentrating in *vacuo*, the remaining residue was taken up in water (20 mL) and the mixture subsequently extracted with EtOAc (3 x 20 mL). The combined organic layers were extracted with aq. 0.5 M HCl (3 x 20 mL) and the separated aqueous layers combined and adjusted to pH 9-10 by

addition of an aq. NH₃ solution. After extraction with DCM (3 x 20 mL), the combined organic layers were washed with brine, dried over MgSO₄, filtered, and finally concentrated in *vacuo* to give crude **15** [0.659 g, 77%, 87% purity (qNMR)] which was used without further purification in the next step.

¹H-NMR (500MHz, DMSO-d₆): δ 1.36 (s, 9H), 1.51 (quint, ³J = 6.9 Hz, 2H), 2.44 (t, ³J = 6.7 Hz, 2H), 2.95 (dt, ³J = 6.6 Hz, ³J = 6.3 Hz, 2H), 3.29 (s, 1H), 3.62 (s, 2H), 6.74 (s, 1H), 7.26 (psd, ³J + ⁵J = 8.6 Hz, 2H), 7.47 (psd, ³J + ⁵J = 8.3 Hz, 2H). ¹³C-NMR (125MHz, DMSO-d₆): δ 28.8, 30.3, 38.7, 46.7, 52.7, 77.9, 119.9, 130.6, 131.4, 141.1, 156.1. MS (ESI+) m/z (%): 342.15 (100) [⁷⁹Br, M+H]⁺, 687.23 (80) [⁷⁹Br, ⁸¹Br, 2M+H]⁺. HRMS (EI): calcd for C₁₅H₂₃BrN₂O₂ [⁷⁹Br, M+H]⁺: 342.094289, found: 342.095397. HRMS-(EI): calcd for C₁₅H₂₃BrN₂O₂ [⁸¹Br, M+H]⁺: 344.092243, found: 344.093534.

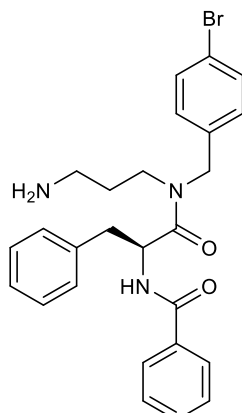
(S)-*tert*-butyl (3-(2-benzamido-*N*-(4-bromobenzyl)-3-phenylpropanamido)propyl)carbamate (**16**)



To a solution of *N*-benzoyl-*L*-phenylalanine (0.498 g, 1.85 mmol), HBTU (0.771 g, 2.04 mmol, 1.1 equiv.) and *N*-methylmorpholine (1.017 ml, 9.25 mmol, 5 equiv.) in 8 ml DMF, **15** (0.699 g, 2.04 mmol, 1.1 equiv.) was added and the reaction mixture stirred at RT for 14h under an argon atmosphere. After addition of DCM (100 mL), the separated organic layer was exhaustively washed with an aqueous 5% LiOH solution (5 x 50 ml), dried over MgSO₄, filtered, and finally concentrated in *vacuo*. Flash chromatography (cyclohexanes/EtOAc, gradient from 0 → 5% over 15 min) of the remaining crude product gave rise to **16** as colorless solid (0.671 g, 61%).

Mp: 130-133°C. ¹H-NMR (500MHz, DMSO-d₆, mixture of rotamers): δ 1.35 (s, 9H), 1.53-1.71 (m, 2H), 2.81-2.96 (m, 2H), 2.98-3.11 (m, 2H), 3.15-3.27 (m, 1H), 4.40-4.73 (m, 2H), 4.97-5.12 (m, 1H), 6.67-6.82 (m, 1H), 7.09-7.31 (m, 6H), 7.32-7.54 (m, 6H), 7.76-7.85 (m, 2H), 8.79-8.82 (m, 1H). ¹³C-NMR (100MHz, CDCl₃, mixture of rotamers): δ 27.5, 28.5, 28.7, 37.3, 37.8, 39.5, 39.9, 43.4, 44.5, 48.4, 50.3, 50.5, 51.2, 79.2, 79.4, 121.5, 121.8, 127.2, 128.5, 128.7, 128.75, 128.77, 129.6, 129.8, 131.8, 131.9, 132.1, 133.7, 133.8, 135.2, 135.8, 136.1, 136.3, 156.1, 156.3, 166.8, 167.0, 171.9, 172.5. MS (ESI+) m/z (%): 594 (100) [⁷⁹Br, M+H]⁺, 596 (100) [⁸¹Br, M+H]⁺. Anal. calcd for: C₃₁H₃₆BrN₃O₄: C, 62.63; H, 6.10; N, 7.07; found: C: 62.68; H, 6.20; N, 7.27.

(S)-*N*-(1-((3-aminopropyl)(4-bromobenzyl)amino)-1-oxo-3-phenylpropan-2-yl)benzamide (**17**)



To a solution of **16** (0.719 g, 1.21 mmol) in DCM (6 mL), TFA (0.419 mL, 5.45 mmol, 4.5 equiv.) was added and the reaction mixture stirred at RT for 72h. The mixture was then quenched by addition of a sat. NaHCO₃ solution (10 mL) and the separated organic layer washed with brine, dried over MgSO₄, filtered, and concentrated in *vacuo*. Flash chromatography (DCM/MeOH gradient from 0 → 10% over 15 min) of the crude product yielded **17** as colorless, hygroscopic solid (0.550 g, 92%).

Mp: 46-50°C (hygroscopic). ¹H-NMR (500MHz, DMSO-d₆, mixture of rotamers): δ 1.70-1.83 (sm, 1.5H), 1.90-2.05 (sm, 0.5H), 2.70 (t, ³J = 7.5 Hz, 1H), 2.78 (t, ³J = 7.2 Hz, 1H), 2.96-3.04 (sm, 1H), 3.07-3.15 (m, 1H), 3.23-3.40 (m, 2H), 3.42-3.49 (sm, 1H), 4.40 (d, ²J = 15.5 Hz, 0.5H), 4.60 (d, ²J = 15.5 Hz, 0.5H), 4.61 (d, ²J = 17.5 Hz, 0.5 H), 4.77 (d, ²J = 17.2 Hz, 0.5H), 4.97 (dd, ²J = 14.1 Hz, ³J = 8.2 Hz, 0.5H), 5.12 (dd, ²J = 14.9 Hz, ³J = 8.0 Hz, 0.5H), 7.09-7.94 (m, 5H), 7.27 (pst, ³J = 7.5 Hz, 1H), 7.37-7.55 (m, 6H), 7.78 (d, ³J = 7.2 Hz, 1H), 7.81-7.92 (m, 3H), 8.86 (d, ³J = 7.5 Hz, 1H). ¹³C-NMR (125MHz, DMSO-d₆): δ 25.8, 27.1, 37.0, 37.2, 37.6, 37.7, 43.7, 45.0, 48.2, 50.2, 51.7, 52.1, 120.5, 120.9, 126.95, 127.02, 128.0, 128.1, 128.65, 128.68, 128.7, 128.8, 129.5, 129.8, 130.0, 130.1, 131.7, 1321.9, 132.0, 134.2, 134.3, 137.4, 137.8, 138.1, 138.3, 166.8, 167.0, 172.1, 127.6. MS (ESI) *m/z* (%): 494.10 (100) [⁷⁹Br, M+H]⁺. HRMS (EI): calcd for C₂₆H₂₈BrN₃O₂ [⁷⁹Br, M+H]⁺: 493.136489, found: 493.138102. HRMS (EI): calcd for C₂₆H₂₈BrN₃O₂: [⁸¹Br, M+H]⁺: 495.134442, found: 495.135035. Anal. calcd for: C₂₆H₂₈BrN₃O₂*2.5 H₂O: C, 57.89; H, 6.17; N, 7.79; found: C: 57.55; H, 5.66; N, 7.70.